

Adaptive non-singular integral terminal sliding mode tracking control for autonomous underwater vehicles

Lei Qiao^{1,2}, Weidong Zhang^{1,2}✉¹*Department of Automation, Shanghai Jiao Tong University, Shanghai 200240, People's Republic of China*²*Key Laboratory of System Control and Information Processing, Ministry of Education, Shanghai 200240, People's Republic of China*

✉ E-mail: wdzhang@sjtu.edu.cn

Abstract: This study proposes an adaptive non-singular integral terminal sliding mode control (ANITSMC) scheme for trajectory tracking of autonomous underwater vehicles (AUVs) with dynamic uncertainties and time-varying external disturbances. The ANITSMC is first proposed for a first-order uncertain non-linear dynamic system to eliminate the singularity problem in conventional terminal sliding mode control (TSMC) and avoid the requirement of the bound information of the lumped system uncertainty. The time taken to reach the equilibrium point from any initial error is guaranteed to be finite. The proposed ANITSMC is then applied to trajectory tracking control of AUVs. It guarantees that the velocity tracking errors locally converge to zero in finite time and after that the position tracking errors locally converge to zero exponentially. The designed ANITSMC of AUVs avoids the requirement of the prior knowledge of the lumped system uncertainty bounds as opposite to the existing globally finite-time stable tracking control (GFTSTC), provides higher tracking accuracy than the existing GFTSTC and adaptive non-singular TSMC (ANTSMC) and offers faster convergence rate and better robustness against dynamic uncertainties and time-varying external disturbances than the adaptive proportional-integral sliding mode control (APISM). Comparative simulation results are presented to validate the superiority of the ANITSMC over the APISM.

1 Introduction

Due to the potential technical superiority, autonomous underwater vehicles (AUVs) have been widely used in commercial, scientific and military applications, such as offshore oil and gas exploration and exploitation, oceanographic observation and bathymetric survey, and obviating torpedoes [1–4]. In these applications, high precise trajectory tracking or path following with fast dynamic response is usually required to accomplish the specific tasks. Regarding the above two motion control problems of AUVs, trajectory tracking control problem has received relatively more attention than path following control problem, since it is concerned with the design of control laws that force the vehicle to reach and follow a time-varying parameterised trajectory [5]. However, it is very challenging to implement fast and accurate trajectory tracking for AUVs because of the difficulties in designing effective trajectory tracking controllers. The main difficulties include highly non-linear, strongly coupled and uncertain properties of the vehicle dynamics as well as the existence of time-varying external disturbances which are hard to measure or estimate in underwater environments [5–7].

Sliding mode control (SMC) is one of the most powerful methods to handle non-linear systems with uncertainties, perturbations and bounded external disturbances [8]. This is mainly due to its strong robustness against system uncertainties and external disturbances [9]. Owing to the above advantage, SMC has been widely used in the trajectory tracking control problem of underwater vehicles, see for example [5, 10–17]. However, these SMC methods are designed based on linear sliding mode (LSM), which can guarantee only the asymptotical errors convergence due to the asymptotical convergence of the LSM manifold, and therefore, a finite-time errors convergence cannot be obtained.

Terminal SMC (TSMC) is designed to achieve the finite-time convergence of the system dynamics [18–20]. The terminal sliding mode (TSM) manifold is a non-linear function of the tracking errors and their derivatives, and then the finite-time convergence could be realised. TSMC has been successfully used in the control of robotic manipulators [21, 22]. Compared to the conventional SMC, the TSMC can give rise to faster convergence rate, better disturbances rejection ability and better robustness against

uncertainties. However, the main drawback of the TSMC is that it suffers from a singularity problem which can result in the unboundedness of the control input [23]. To solve the singularity problem of the TSMC, some non-singular TSMC (NTSMC) methods are proposed in the works of [24–28]. In [24], an NTSMC is presented for rigid robotic manipulators by combining a new non-singular TSM (NTSM) and a discontinuous reaching law. With this NTSMC method, the singularity problem is totally avoided, but the actuators suffer from chattering due to using the discontinuous reaching law. By improving the NTSM proposed in [24] and utilising a fast TSM-type reaching law, a continuous NTSMC for rigid manipulators is proposed in [25]. Compared with the NTSMC in [24], the advantage of the continuous NTSMC is that it can not only avoid the singularity problem but also eliminate the chattering. However, the disadvantage of the continuous NTSMC is that it reduces the tracking precision due to that the tracking errors can only be guaranteed to converge to bounded fields. Using an NTSM and a time-delay estimation (TDE) algorithm, a practical NTSMC for robot manipulator is presented in [26]. The proposed controller needs no detailed information about the robot dynamics due to the TDE and ensures fast convergence due to the NTSM. Through three degree-of-freedom programmable universal machine for assembly (PUMA) type robot experiments, the expected performance of the proposed controller is verified. Based on the practical NTSMC proposed in [26], a continuous fractional-order NTSMC (FONTSMC) for robot manipulators is proposed in [27] by using the TDE algorithm and fast TSM-type reaching law. Compared with the practical NTSMC in [26], the FONTSMC ensures better control performance in a wide range of speed. To eliminate the reaching phase, a time-varying NTSMC for robot manipulators is proposed in [28] by incorporating a piecewise defined function of time into an NTSM manifold. Under this controller, the robustness is guaranteed during the entire response of the system and the convergent time can be chosen in advance. This controller is subsequently modified to ensure faster convergence rate and smaller control input. As a new form of singular-free TSMC, integral TSMC (ITSMC) is recently proposed in [29, 30]. In [29], the ITSMC is developed for a class of multi input multi output (MIMO) uncertain non-linear system by

introducing sign and fractional integral TSM (ITSM). The singularity problem is avoided and the reaching phase is eliminated. The application on a two-link robot manipulator control verifies the effectiveness of the ITSMC. Inspired by the ITSM given in [29], a global fast non-singular ITSMC (FNITSMC) for a class of non-linear system with uncertainties and disturbances is proposed in [30]. In contrast to the ITSMC in [29], the FNITSMC improves the convergence rate. Through simulating the control method on a two-link rigid robot manipulator, the expected performance of the FNITSMC is demonstrated.

Although the aforementioned NTSMC and ITSMC methods are widely used in the control of robotic manipulators, there are few results in the control of underwater vehicles. Recently, [6] proposes a globally finite-time stable tracking control (GFTSTC) strategy for the horizontal motion of unmanned underwater vehicles (UUVs) via ITSMC and proportional-integral-derivative SMC (PIDSMC). This control strategy can guarantee globally finite-time convergence of the position and velocity tracking errors to the bounded neighbourhood of the origin without any singularity in the presence of parameter perturbation and unknown constant disturbances. Nevertheless, the tracking errors cannot be guaranteed to converge to zero and the bound information of the parameter perturbation is needed in the controller design. [31] presents a multivariable output feedback adaptive NTSMC (ANTSMC) strategy for three-dimensional trajectory tracking control of underwater vehicles with parameter uncertainties and external disturbances. This control strategy can not only guarantee the position and velocity tracking errors to locally converge to bounded small fields in finite time but also remove the requirement of the bound information of the parameter uncertainties and external disturbances by using adaptive technology. However, as the GFTSTC in [6], the tracking errors also cannot be ensured to converge to zero.

In this paper, a novel adaptive non-singular ITSMC (ANITSMC) scheme is proposed for trajectory tracking of AUVs with dynamic uncertainties and time-varying external disturbances. The ANITSMC is first presented in the theoretical part to stabilise a first-order uncertain non-linear dynamic system. It guarantees that the tracking error converges to zero in finite time from any initial value. The singularity problem in conventional TSMC is overcome and the prior knowledge of the upper bound of the lumped system uncertainty is not required by introducing an adaptive mechanism to estimate the parameters of the lumped system uncertainty bounds. The ANITSMC for trajectory tracking control of AUVs is then given in the application part. It is shown that under the proposed ANITSMC scheme, the velocity tracking errors locally converge to zero in finite time and after that the position tracking errors locally converge to zero exponentially. Unlike the GFTSTC [6], the proposed ANITSMC of AUVs does not need the prior knowledge of the upper bound of the lumped system uncertainty. With respect to the GFTSTC [6] and ANTSMC [31], the proposed ANITSMC of AUVs offers higher tracking accuracy. If the fractional powers of the proposed ANITSMC are taken as 1, this control scheme will reduce to the corresponding adaptive proportional-integral SMC (APISM) scheme. In contrast to this reduced controller, faster convergence rate and better robustness against dynamic uncertainties and time-varying external disturbances are obtained for trajectory tracking control of AUVs. Numerical simulations performed on a fully actuated AUV demonstrate the expected performances of the ANITSMC compared with the APISM.

This paper is organised as follows. In Section 2, some useful notations and preliminaries are given. In Section 3, the ANITSMC for a first-order uncertain non-linear dynamic system is designed. In Section 4, the ANITSMC applied to trajectory tracking control of AUVs is presented. To show the effectiveness of the proposed approach, comparative simulations between the ANITSMC and the APISM are performed in Section 5. Finally, conclusions are made in Section 6.

2 Notations and preliminaries

2.1 Notations

Throughout this paper, the following notations are used. For a vector $\vartheta \in R^n$, denote $\vartheta^{\varpi_1/\varpi_2} = [|\vartheta_1|^{\varpi_1/\varpi_2} sgn(\vartheta_1), \dots, |\vartheta_n|^{\varpi_1/\varpi_2} sgn(\vartheta_n)]^T$ where ϖ_1, ϖ_2 are positive odd integers and $sgn(\cdot)$ is the standard sign function, denote $\text{diag}(\vartheta) = \text{diag}(\vartheta_1, \dots, \vartheta_n)$ where $\text{diag}(\cdot)$ is the diagonal matrix, $\max_{i=1,\dots,n}(\vartheta_i)$ is denoted as the largest element in ϑ , the norm of vector ϑ is defined as the Euclidean norm, i.e. $\|\vartheta\| = \sqrt{\vartheta^T \vartheta}$. For a matrix $A \in R^{n \times n}$, $\lambda_{\max}(A)$ and $\lambda_{\min}(A)$ are denoted as the largest and smallest eigenvalues of matrix A , respectively, the norm of matrix A is defined as the induced 2-norm, i.e. $\|A\| = \sqrt{\lambda_{\max}(A^T A)}$.

2.2 Preliminaries

Lemma 1 [32]: Consider the system

$$\dot{x} = f(\bar{x}), \quad f(0) = 0, \quad \bar{x} \in R^n, \quad \bar{x}(0) = \bar{x}_0 \quad (1)$$

where $f: D \rightarrow R^n$ is continuous on an open neighbourhood D of the origin $\bar{x} = 0$. Let $\bar{x} = 0$ be an equilibrium point for system (1). Suppose there exist a continuously differentiable function $V(\bar{x}): D \rightarrow R$, real numbers $\bar{\varepsilon} > 0$ and $\gamma \in (0, 1)$, and an open neighbourhood $U \subset D$ of the origin such that

$$V(\bar{x}) > 0, \quad \forall \bar{x} \neq 0 \quad (2)$$

$$\dot{V}(\bar{x}) + \bar{\varepsilon} V'(\bar{x}) \leq 0, \quad \bar{x} \in U \setminus \{0\}. \quad (3)$$

Then, the origin $\bar{x} = 0$ is a finite-time stable equilibrium point of system (1). In addition, the finite settling time T satisfies

$$T \leq \frac{V^{1-\gamma}(\bar{x}_0)}{\bar{\varepsilon}(1-\gamma)}. \quad (4)$$

3 Adaptive non-singular integral terminal sliding mode control

3.1 ANITSMC design

In this section, an ANITSMC scheme is proposed for a first-order uncertain non-linear dynamic system to track the desired trajectory with high robustness and fast convergence rate.

Consider a first-order non-linear dynamic system with uncertainty and external disturbance described below

$$\dot{x}(t) = \hat{f}(x(t)) + \tilde{f}(x(t)) + d(t) + bu(t) \quad (5)$$

where $x(t) \in R$ is the system state, $\hat{f}(x(t))$ is the nominal dynamic function, $\tilde{f}(x(t))$ is the uncertain dynamic function representing the unmodelled dynamics or structural variation of the system (5), $d(t)$ is the unknown external disturbance, $u(t)$ is the control input and b is a known constant.

Assumption 1: The dynamic uncertainty $\tilde{f}(x(t))$ and the external disturbance $d(t)$ are upper bounded in the following form:

$$\begin{aligned} |\tilde{f}(x(t))| &< l_0 + l_1|x(t)| + l_2|x(t)|^2, \\ |d(t)| &< l_3 \end{aligned} \quad (6)$$

in which l_i ($i = 0, \dots, 3$) are unknown positive constants.

Let $L(\tilde{f}(x(t)), d(t)) = \tilde{f}(x(t)) + d(t)$ be the lumped system uncertainty, then, according to (6), $L(\tilde{f}(x(t)), d(t))$ can be upper bounded in the following fashion:

$$\begin{aligned}
|L(\tilde{f}(x(t)), d(t))| &= |\tilde{f}(x(t)) + d(t)| \\
&\leq |\tilde{f}(x(t))| + |d(t)| \\
&< (l_0 + l_3) + l_1|x(t)| + l_2|x(t)|^2 \\
&= h_0 + h_1|x(t)| + h_2|x(t)|^2
\end{aligned} \tag{7}$$

where $h_0 = l_0 + l_3$, $h_1 = l_1$ and $h_2 = l_2$ are all unknown positive constants.

The control objective is to design the control input $u(t)$ such that $x(t)$ precisely tracks the desired trajectory $x_d(t) \in R$ in finite time without the requirement of the prior knowledge of the bound parameters h_i ($i = 0, 1, 2$) of the lumped system uncertainty in (7).

To design robust control system with the tracking error convergence in finite time, we define the following non-singular ITSM (NITSM) manifold

$$s(t) = \int_0^t e(\tau) d\tau + \alpha e^{p_1/p_2}(t) \tag{8}$$

where $e(t) = x(t) - x_d(t)$ is the tracking error, $\alpha > 0$ is a design constant, and p_1 and p_2 are positive odd integers satisfying $1 < p_1/p_2 < 2$.

Remark 1: The selection of parameters p_1 and p_2 in (8) is a key problem in the TSMC. Here we choose p_1 and p_2 satisfying the above conditions to achieve two purposes: (i) to guarantee that the tracking error $e(t)$ can converge to zero on the NITSM manifold $s(t) = 0$ in finite time and (ii) to avoid the singularity problem in the controller design. The details are given later.

With the NITSM manifold defined above, now the ANITSMC scheme is designed in the following theorem.

Theorem 1: For system (5) with the NITSM manifold (8), if the controller is designed as

$$u(t) = -b^{-1}(\hat{f}(x(t)) - \dot{x}_d(t) + \alpha^{-1} \frac{p_2}{p_1} e^{2-p_1/p_2}(t) + u_1(t)) \tag{9}$$

$$u_1(t) = \begin{cases} \frac{s(t)}{|s(t)|} (\hat{h}_0 + \hat{h}_1|x(t)| + \hat{h}_2|x(t)|^2), & \text{for } |s(t)| \neq 0 \\ 0, & \text{for } |s(t)| = 0 \end{cases} \tag{10}$$

where \hat{h}_i ($i = 0, 1, 2$) are the estimates of h_i ($i = 0, 1, 2$) and they are updated by the following adaptation laws:

$$\dot{\hat{h}}_0 = \rho_0 \alpha \frac{p_1}{p_2} e^{p_1/p_2-1}(t) |s(t)| \tag{11}$$

$$\dot{\hat{h}}_1 = \rho_1 \alpha \frac{p_1}{p_2} e^{p_1/p_2-1}(t) |s(t)| |x(t)| \tag{12}$$

$$\dot{\hat{h}}_2 = \rho_2 \alpha \frac{p_1}{p_2} e^{p_1/p_2-1}(t) |s(t)| |x(t)|^2 \tag{13}$$

in which ρ_i ($i = 0, 1, 2$) are positive constants that determine the rate of adaptation, and $\hat{h}_i(0) > 0$ for all $i = 0, 1, 2$, then, the tracking error $e(t)$ will converge to zero in finite time from any initial value.

The proof of this theorem is shown in the next section.

3.2 Stability analysis

Before the proof of Theorem 1, the following useful lemma is firstly given.

Lemma 2: Given the uncertain non-linear dynamic system (5) with the NITSM variable $s(t)$ (8) controlled by (9)–(13), the gains \hat{h}_i

($i = 0, 1, 2$) in (10) have upper bounds, i.e. there exist positive constants $h_i^\#$ ($i = 0, 1, 2$) such that

$$\hat{h}_i \leq h_i^\#, \quad i = 0, 1, 2. \tag{14}$$

Proof: The proof of this lemma is based on the proof of Lemma 1 of [33]. Suppose that $e(t) \neq 0$ and $s(t) \neq 0$, from the update laws of \hat{h}_i ($i = 0, 1, 2$) expressed in (11)–(13), and given that h_i ($i = 0, 1, 2$) are bounded, it follows that \hat{h}_i ($i = 0, 1, 2$) are increasing and there exists a time t_1 such that $\hat{h}_i(t_1) > h_i$ for $i = 0, 1, 2$. Note that these gains have finite values by the absolute continuity property of \hat{h}_i ($i = 0, 1, 2$). From $t = t_1$, the gains \hat{h}_i ($i = 0, 1, 2$) are large enough to make the NITSM variable $s(t)$ decreasing. Then, it yields that, in a finite time t_2 , $s(t_2) = 0$ and $\hat{h}_i(t_2)$ ($i = 0, 1, 2$) admit bounded values. It yields that there always exist positive constants $h_i^\#$ ($i = 0, 1, 2$) such that $h_i^\# \geq \hat{h}_i$ for $i = 0, 1, 2$. On the other hand, for the case of $e(t) = 0$ and $s(t) \neq 0$, from (5), (9) and (10) we have

$$\begin{aligned}
\dot{e}(t) &= \dot{x}(t) - \dot{x}_d(t) \\
&= \hat{f}(x(t)) + L(\tilde{f}(x(t)), d(t)) + bu(t) - \dot{x}_d(t) \\
&= -\frac{s(t)}{|s(t)|} (\hat{h}_0 + \hat{h}_1|x(t)| + \hat{h}_2|x(t)|^2) + L(\tilde{f}(x(t)), d(t)).
\end{aligned} \tag{15}$$

Assume that $e(t) \equiv 0$, it follows from (8), (11)–(13) that $\dot{s}(t) = e(t) + (\alpha p_1/p_2) e^{p_1/p_2-1}(t) \dot{e}(t) \equiv 0$ and $\dot{\hat{h}}_i \equiv 0$ ($i = 0, 1, 2$), which implies that $s(t)$ and \hat{h}_i ($i = 0, 1, 2$) are all constants. According to (15) and the arbitrariness of the external disturbance $d(t)$, we have $\dot{e}(t) \not\equiv 0$ and consequently $e(t) \not\equiv 0$, which is in contradiction with the initial assumption of $e(t) \equiv 0$. Therefore, we obtain $e(t) \not\equiv 0$, showing that $e(t) = 0$ does not hinder the reachability of the NITSM manifold $s(t) = 0$. Thus, the gains \hat{h}_i ($i = 0, 1, 2$) will continue to increase until the NITSM variable $s(t)$ converges to zero. After that, \hat{h}_i ($i = 0, 1, 2$) will admit bounded values and as a consequence, the boundedness of \hat{h}_i ($i = 0, 1, 2$) is guaranteed, i.e. the inequalities (14) hold for some positive constants $h_i^\#$ ($i = 0, 1, 2$). This completes the proof. \square

With Lemmas 1 and 2 given above, now the proof of Theorem 1 is ready to be given.

Proof of Theorem 1: From Lemma 2, there always exist positive constants h_i^* ($i = 0, 1, 2$) such that $h_i^* > h_i$ and $h_i^* > \hat{h}_i$ for all $i = 0, 1, 2$. Let $\tilde{h}_i = \hat{h}_i - h_i^*$ for $i = 0, 1, 2$, inspired by [33], consider the following Lyapunov function:

$$V = \frac{1}{2} s^2(t) + \frac{1}{2} \sum_{i=0}^2 \beta_i^{-1} \tilde{h}_i^2 \tag{16}$$

where β_i ($i = 0, 1, 2$) are positive constants satisfying $\beta_i < \rho_i$.

By differentiating V with respect to time, using (5), (8) and (9), it can be obtained that

$$\begin{aligned}
\dot{V} &= s(t) \dot{s}(t) + \sum_{i=0}^2 \beta_i^{-1} \tilde{h}_i \dot{\tilde{h}}_i \\
&= s(t)(e(t) + \alpha \frac{p_1}{p_2} e^{p_1/p_2-1}(t) \dot{e}(t)) + \sum_{i=0}^2 \beta_i^{-1} \tilde{h}_i \dot{\tilde{h}}_i \\
&= s(t)(e(t) + \alpha \frac{p_1}{p_2} e^{p_1/p_2-1}(t)(\dot{x}(t) - \dot{x}_d(t))) + \sum_{i=0}^2 \beta_i^{-1} \tilde{h}_i \dot{\tilde{h}}_i.
\end{aligned} \tag{17a}$$

$$\begin{aligned}
&= s(t)(e(t) + \alpha \frac{p_1}{p_2} e^{p_1/p_2 - 1}(t)(\hat{f}(x(t))) \\
&\quad + \tilde{L}(\tilde{f}(x(t)), d(t)) + bu(t) - \dot{x}_d(t))) + \sum_{i=0}^2 \beta_i^{-1} \tilde{h}_i \dot{\tilde{h}}_i \\
&= \alpha \frac{p_1}{p_2} e^{p_1/p_2 - 1}(t)s(t)L(\tilde{f}(x(t)), d(t)) \\
&\quad - \alpha \frac{p_1}{p_2} e^{p_1/p_2 - 1}(t)s(t)u_i(t) + \sum_{i=0}^2 \beta_i^{-1} \tilde{h}_i \dot{\tilde{h}}_i
\end{aligned} \tag{17b}$$

For the case of $e(t) \neq 0$ and $s(t) \neq 0$, noting that $\dot{\tilde{h}}_i = \dot{\tilde{h}}_i$ ($i = 0, 1, 2$), which together with (7) and (10)–(13) allow us to obtain

$$\begin{aligned}
\dot{V} &= \alpha \frac{p_1}{p_2} e^{p_1/p_2 - 1}(t)s(t)L(\tilde{f}(x(t)), d(t)) \\
&\quad - \alpha \frac{p_1}{p_2} e^{p_1/p_2 - 1}(t)|s(t)|(|\hat{h}_0 + \hat{h}_1|x(t)| + \hat{h}_2|x(t)|^2) \\
&\quad + \alpha \frac{p_1}{p_2} e^{p_1/p_2 - 1}(t)|s(t)|(\beta_0^{-1}\rho_0(\hat{h}_0 - h_0^*)) \\
&\quad + \beta_1^{-1}\rho_1|x(t)||(\hat{h}_1 - h_1^*) + \beta_2^{-1}\rho_2|x(t)|^2(\hat{h}_2 - h_2^*)
\end{aligned} \tag{18a}$$

$$\begin{aligned}
&\leq \alpha \frac{p_1}{p_2} e^{p_1/p_2 - 1}(t)|s(t)|(h_0 + h_1|x(t)| + h_2|x(t)|^2) \\
&\quad - \alpha \frac{p_1}{p_2} e^{p_1/p_2 - 1}(t)|s(t)|(h_0^* + h_1^*|x(t)| + h_2^*|x(t)|^2) \\
&\quad + \alpha \frac{p_1}{p_2} e^{p_1/p_2 - 1}(t)|s(t)|(h_0^* + h_1^*|x(t)| + h_2^*|x(t)|^2) \\
&\quad - \alpha \frac{p_1}{p_2} e^{p_1/p_2 - 1}(t)|s(t)|(\hat{h}_0 + \hat{h}_1|x(t)| + \hat{h}_2|x(t)|^2) \\
&\quad + \alpha \frac{p_1}{p_2} e^{p_1/p_2 - 1}(t)|s(t)|(\beta_0^{-1}\rho_0(\hat{h}_0 - h_0^*)) \\
&\quad + \beta_1^{-1}\rho_1|x(t)||(\hat{h}_1 - h_1^*) + \beta_2^{-1}\rho_2|x(t)|^2(\hat{h}_2 - h_2^*)
\end{aligned} \tag{18b}$$

$$\begin{aligned}
&= -\alpha \frac{p_1}{p_2} e^{p_1/p_2 - 1}(t)((h_0^* - h_0) + (h_1^* - h_1)|x(t)| \\
&\quad + (h_2^* - h_2)|x(t)|^2)|s(t)| \\
&\quad + \alpha \frac{p_1}{p_2} e^{p_1/p_2 - 1}(t)|s(t)|((h_0^* - \hat{h}_0) + (h_1^* - \hat{h}_1)|x(t)| \\
&\quad + (h_2^* - \hat{h}_2)|x(t)|^2)
\end{aligned} \tag{18c}$$

$$\begin{aligned}
&= -\alpha \frac{p_1}{p_2} e^{p_1/p_2 - 1}(t)((h_0^* - h_0) + (h_1^* - h_1)|x(t)| \\
&\quad + (h_2^* - h_2)|x(t)|^2)|s(t)| \\
&\quad - \alpha \frac{p_1}{p_2} e^{p_1/p_2 - 1}(t)|s(t)|(\beta_0^{-1}\rho_0(h_0^* - \hat{h}_0)) \\
&\quad + \beta_1^{-1}\rho_1|x(t)||(\hat{h}_1 - h_1^*) + \beta_2^{-1}\rho_2|x(t)|^2(h_2^* - \hat{h}_2)) \\
&= -\alpha \frac{p_1}{p_2} e^{p_1/p_2 - 1}(t)((h_0^* - h_0) + (h_1^* - h_1)|x(t)| \\
&\quad + (h_2^* - h_2)|x(t)|^2)|s(t)| \\
&\quad - \alpha \frac{p_1}{p_2} e^{p_1/p_2 - 1}(t)|s(t)|(\beta_0^{-1}\rho_0 - 1)(h_0^* - \hat{h}_0) \\
&\quad - \alpha \frac{p_1}{p_2} e^{p_1/p_2 - 1}(t)|s(t)|(\beta_1^{-1}\rho_1 - 1)|x(t||(\hat{h}_1 - h_1^*) \\
&\quad - \alpha \frac{p_1}{p_2} e^{p_1/p_2 - 1}(t)|s(t)|(\beta_2^{-1}\rho_2 - 1)|x(t)|^2(h_2^* - \hat{h}_2))
\end{aligned} \tag{18d}$$

Let

$$\begin{aligned}
\Delta_1 &= \alpha \frac{p_1}{p_2} e^{p_1/p_2 - 1}(t)((h_0^* - h_0) + (h_1^* - h_1)|x(t)| + (h_2^* - h_2)|x(t)|^2), \\
\Delta_2 &= \alpha \frac{p_1}{p_2} e^{p_1/p_2 - 1}(t)|s(t)|(\beta_0^{-1}\rho_0 - 1), \\
\Delta_3 &= \alpha \frac{p_1}{p_2} e^{p_1/p_2 - 1}(t)|s(t)|(\beta_1^{-1}\rho_1 - 1)|x(t)|, \\
\Delta_4 &= \alpha \frac{p_1}{p_2} e^{p_1/p_2 - 1}(t)|s(t)|(\beta_2^{-1}\rho_2 - 1)|x(t)|^2.
\end{aligned} \tag{19}$$

Then, from (16), (18) and (19) we have

$$\begin{aligned}
\dot{V} &\leq -\sqrt{2}\Delta_1 \frac{\sqrt{2}}{2}|s(t)| - \sqrt{2\beta_0}\Delta_2 \frac{\sqrt{2}}{2\sqrt{\beta_0}}(h_0^* - \hat{h}_0) \\
&\quad - \sqrt{2\beta_1}\Delta_3 \frac{\sqrt{2}}{2\sqrt{\beta_1}}(h_1^* - \hat{h}_1) - \sqrt{2\beta_2}\Delta_4 \frac{\sqrt{2}}{2\sqrt{\beta_2}}(h_2^* - \hat{h}_2) \\
&\leq -\min(\sqrt{2}\Delta_1, \sqrt{2\beta_0}\Delta_2, \sqrt{2\beta_1}\Delta_3, \sqrt{2\beta_2}\Delta_4) \left(\frac{\sqrt{2}}{2}|s(t)| \right. \\
&\quad \left. + \frac{\sqrt{2}}{2\sqrt{\beta_0}}(h_0^* - \hat{h}_0) + \frac{\sqrt{2}}{2\sqrt{\beta_1}}(h_1^* - \hat{h}_1) + \frac{\sqrt{2}}{2\sqrt{\beta_2}}(h_2^* - \hat{h}_2) \right) \\
&\leq -\omega V^{1/2}
\end{aligned} \tag{20}$$

where

$$\omega = \min(\sqrt{2}\Delta_1, \sqrt{2\beta_0}\Delta_2, \sqrt{2\beta_1}\Delta_3, \sqrt{2\beta_2}\Delta_4) > 0.$$

Therefore, according to Lemma 1, the NITSM manifold $s(t) = 0$ can be reached in the finite time

$$t_s \leq \frac{2V^{1/2}}{\omega}. \tag{21}$$

For the case of $e(t) = 0$ and $s(t) \neq 0$, it has been shown in the proof of Lemma 2 that $e(t) = 0$ is not an attractor in the reaching phase. Hence, the reachability of the NITSM manifold $s(t) = 0$ in the finite time (21) is still ensured.

On the NITSM manifold $s(t) = 0$, we have

$$\int_0^t e(\tau) d\tau = -\alpha e^{p_1/p_2}(t). \tag{22}$$

Taking the time derivative on both sides of (22) leads to

$$\dot{e}(t) = -\alpha^{-1} \frac{p_2}{p_1} e^{2-p_1/p_2}(t). \tag{23}$$

Solving the error dynamic equation (23) yields

$$e(t) = (e^{p_1/p_2 - 1}(t_s) - \alpha^{-1}(1 - p_2/p_1)(t - t_s))^{1/(p_1/p_2 - 1)}. \tag{24}$$

Then the convergent time t_f that is taken to travel from $e(t_s)$ to $e(t_s + t_f) = 0$ can be calculated as

$$t_f = \frac{\alpha}{(1 - p_2/p_1)} |e(t_s)|^{p_1/p_2 - 1}. \tag{25}$$

Thus, the total convergent time t_r spent from $e(0)$ to $e(t_r) = 0$ will be the sum of t_s and t_f , i.e.

$$t_r = t_s + t_f. \tag{26}$$

This completes the proof. \square

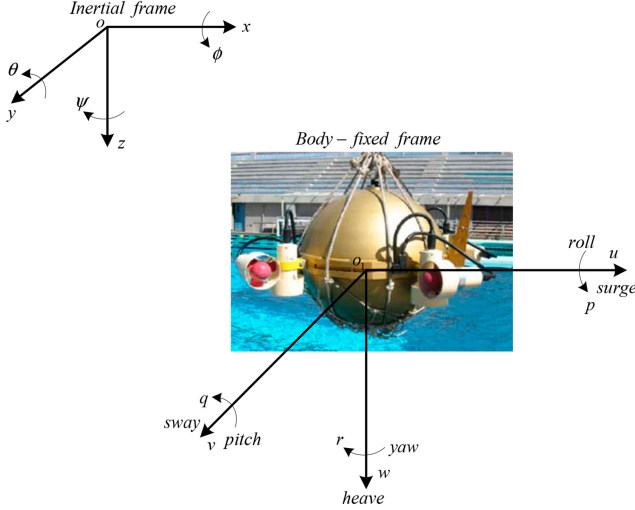


Fig. 1 Inertial and body-fixed coordinate frames for an AUV

Remark 2: Since $1 < p_1/p_2 < 2$, we can obtain that $0 < 2 - p_1/p_2 < 1$ and $0 < p_1/p_2 - 1 < 1$, then $e^{p_1/p_2-1}(t)$ in adaptation laws (11)–(13) and $e^{2-p_1/p_2}(t)$ in the control law (9) will not be equal to infinity, and thus the designed ANITSMC scheme is non-singular.

Remark 3: The prior knowledge of the upper bound of the lumped system uncertainty $L(\tilde{f}(x(t)), d(t))$ is not required in the ANITSMC scheme design. Adaptation laws (11)–(13) are introduced to estimate the parameters of the lumped system uncertainty bounds. The estimates are then used as control parameters of control law (10). When the tracking error is large due to the effects of the lumped system uncertainty, \hat{h}_i ($i = 0, 1, 2$), namely the estimates of h_i ($i = 0, 1, 2$), can be adaptively increased according to the adaptation laws (11)–(13). The amplitude of the control gains can then be increased until the NITSM variable $s(t)$ in (8) converges to zero. After that, \hat{h}_i ($i = 0, 1, 2$) become constants which can keep the error trajectory on the NITSM manifold $s(t) = 0$. Thus, the effects of the lumped system uncertainty can be eliminated and the finite-time tracking error convergence on the NITSM manifold can be guaranteed.

4 Adaptive non-singular integral terminal sliding mode control for trajectory tracking of AUVs

In this section, the proposed ANITSMC scheme is extended to control the MIMO AUV systems to track the desired trajectory in the presence of dynamic uncertainties and time-varying external disturbances. Before the ANITSMC scheme design, the system modelling of the AUV is firstly conducted.

4.1 AUV kinematic and dynamic models

The general kinematic and dynamic models of an AUV moving in three-dimensional space can be developed using the inertial coordinate frame and the body-fixed coordinate frame as shown in Fig. 1. Let $\eta = [x, y, z, \phi, \theta, \psi]^T$ be the position and attitude of the vehicle with respect to the inertial frame and $v = [u, v, w, p, q, r]^T$ be the linear and angular velocities of the vehicle with respect to the body-fixed frame, then the kinematic model of the AUV relating the body-fixed frame to the inertial frame can be expressed as [34]

$$\dot{\eta} = J(\eta)v \quad (27)$$

where $J(\eta) \in R^{6 \times 6}$ is the transformation matrix between the inertial frame and the vehicle's body-fixed frame and it is defined as

$$J(\eta) = \begin{bmatrix} J_1(\eta) & 0_{3 \times 3} \\ 0_{3 \times 3} & J_2(\eta) \end{bmatrix}. \quad (28)$$

In (28), $J_1: R^6 \rightarrow R^{3 \times 3}$ and $J_2: R^6 \rightarrow R^{3 \times 3}$ are defined as

$$J_1(\eta) = \begin{bmatrix} c\psi c\theta & -s\psi c\phi + c\psi s\theta s\phi & s\psi s\phi + c\psi c\phi s\theta \\ s\psi c\theta & c\psi c\phi + s\psi s\theta s\phi & -c\psi s\phi + s\psi c\phi s\theta \\ -s\theta & c\theta s\phi & c\theta c\phi \end{bmatrix},$$

$$J_2(\eta) = \begin{bmatrix} 1 & s\phi t\theta & c\phi t\theta \\ 0 & c\phi & -s\phi \\ 0 & s\phi/c\theta & c\phi/c\theta \end{bmatrix}$$

in which the symbols $s \cdot$, $c \cdot$ and $t \cdot$ denote $\sin(\cdot)$, $\cos(\cdot)$ and $\tan(\cdot)$, respectively, and $0_{3 \times 3} \in R^{3 \times 3}$ represents a matrix of zeros.

Assumption 2 [35]: The transformation matrix $J(\eta)$ is bounded, i.e. there exists an unknown positive constant \bar{J} such that $\| J(\eta) \| \leq \bar{J}$.

Remark 4: It has been shown in [36] that AUVs are not likely to enter the neighbourhood of $\theta = \pm \pi/2$ due to the metacentric restoring forces, thus Assumption 2 is reasonable.

The dynamic model of the AUV in the body-fixed frame can be described as [34]

$$M\ddot{v} + C(v)\dot{v} + D(v)v + g(\eta) + \tau_d = \tau_v \quad (29)$$

where $M \in R^{6 \times 6}$ is the inertia matrix including the added mass, $C(v) \in R^{6 \times 6}$ is the matrix of Coriolis and centripetal forces, $D(v) \in R^{6 \times 6}$ is the matrix of hydrodynamic damping terms, $g(\eta) \in R^6$ is the vector of restoring forces (gravity and buoyancy), $\tau_d \in R^6$ is the vector of time-varying external disturbances and $\tau_v \in R^6$ is the vector of the control input.

As mentioned earlier, the precise dynamic model of the AUV is difficult to obtain due to the non-linear hydrodynamic effects and parameter uncertainties which are hard to measure or estimate accurately in practical applications. These include inertial uncertainties, hydrodynamic coefficients uncertainties and uncertainties in gravity and buoyancy. Therefore, the system dynamic parameters M , $C(v)$, $D(v)$ and $g(\eta)$ given in (29) can be written as the sum of nominal dynamics and dynamic uncertainties

$$\begin{aligned} M &= \hat{M} + \tilde{M}, \\ C(v) &= \hat{C}(v) + \tilde{C}(v), \\ D(v) &= \hat{D}(v) + \tilde{D}(v), \\ g(\eta) &= \hat{g}(\eta) + \tilde{g}(\eta) \end{aligned} \quad (30)$$

where \hat{M} , $\hat{C}(v)$, $\hat{D}(v)$ and $\hat{g}(\eta)$ are the nominal terms and \tilde{M} , $\tilde{C}(v)$, $\tilde{D}(v)$ and $\tilde{g}(\eta)$ are the uncertain terms. Then, the dynamic model of the AUV given in (29) can be rewritten as the following form:

$$\hat{M}\ddot{v} + \hat{C}(v)\dot{v} + \hat{D}(v)v + \hat{g}(\eta) = \tau_v + \tau_{d\eta} \quad (31)$$

where $\tau_{d\eta}$ is the lumped system uncertainty which is defined as

$$\tau_{d\eta} = -\tilde{M}\ddot{v} - \tilde{C}(v)\dot{v} - \tilde{D}(v)v - \tilde{g}(\eta) - \tau_d. \quad (32)$$

The following assumptions are made about the AUV dynamics.

Assumption 3: The time-varying external disturbances vector τ_d is bounded, i.e. there exists an unknown positive constant l_d such that $\| \tau_d \| < l_d$.

Based on Assumption 3 and the assumption made by [37] on the upper bound of the lumped uncertainty of the underwater vehicle, the following assumption can be made.

Assumption 4: If the thrust forces do not always exceed the thruster saturation limits and Assumption 3 holds, the lumped system uncertainty $\tau_{d\eta}$ can be upper bounded by the following function:

$$\|\tau_{d\eta}\| < \lambda_0 + \lambda_1 \|v\| + \lambda_2 \|v\|^2 \quad (33)$$

where $\lambda_i (i = 0, 1, 2)$ are unknown positive constants.

Remark 5: The upper bound of the lumped system uncertainty $\tau_{d\eta}$ is indeed input related due to that $\tau_{d\eta}$ contains the acceleration signal \ddot{v} which is input related. However, it has been shown in [37] that when the thrust saturation effect is not serious, the inequality (33) can be satisfied. On the other hand, if the trajectory which always needs more thrust forces than the thruster saturation limits, the inequality (33) may not be satisfied. In this case, adaptive modification of target trajectory or pseudo-control hedging strategy as suggested in [37] can be applied into the controller design to solve the thruster saturation problem. In this paper, like in [37], we choose the trajectories which only require the thrust forces to violate the thruster saturation limits sometimes, thus there always exist some unknown positive constants $\lambda_i (i = 0, 1, 2)$ such that inequality (33) holds.

4.2 ANITSMC design for AUVs

In this section, the development of the ANITSMC scheme for trajectory tracking of AUVs is presented. First, a virtual velocity control command is designed by using the desired position trajectory and position tracking errors. Then, the NITSM manifold which is consisted of integral and fractional velocity tracking errors is developed. At last, by adopting an adaptive technique to estimate and compensate for the dynamic uncertainties and time-varying external disturbances, the ANITSMC scheme is derived, which guarantees that the velocity tracking errors locally converge to zero in finite time and after that the position tracking errors locally converge to zero exponentially.

Let $\eta_d \in R^6$ be the desired position trajectory of the AUV in the inertial frame, the position tracking errors $\tilde{\eta}$ are defined as

$$\tilde{\eta} = \eta - \eta_d. \quad (34)$$

Define the virtual velocity control command v_c as

$$v_c = J^{-1}(\eta)\dot{\eta}_d - J^{-1}(\eta)(K_1\tilde{\eta} + K_2 \int_0^t \tilde{\eta} d\tau) \quad (35)$$

where $K_1 = \text{diag}(k_{11}, \dots, k_{16})$, $K_2 = \text{diag}(k_{21}, \dots, k_{26})$, and k_{1i} and k_{2i} are positive constants satisfying $k_{1i}^2 - 4k_{2i} \geq 0$ for $i = 1, \dots, 6$.

The velocity tracking errors \tilde{v} are defined as

$$\tilde{v} = v - v_c. \quad (36)$$

To achieve the finite-time convergence of the velocity tracking errors \tilde{v} , the NITSM manifold is defined as

$$s_v = \int_0^t \tilde{v} d\tau + K_3 \tilde{v}^{q_1/q_2} \quad (37)$$

where $K_3 = \text{diag}(k_{31}, \dots, k_{36})$, $k_{3i} (i = 1, \dots, 6)$ are positive constants, and q_1 and q_2 are positive odd integers satisfying $1 < q_1/q_2 < 2$.

With the NITSM manifold defined above, now the ANITSMC scheme for AUVs is given in the following theorem.

Theorem 2: For the AUV systems described by (27) and (31) with the NITSM manifold defined in (37), if the control scheme is designed as

$$\tau_v = \tau_0 + \tau_1 + \tau_2 \quad (38)$$

$$\tau_0 = \hat{M}\dot{v}_c + \hat{C}(v)v + \hat{D}(v)v + \hat{g}(\eta) \quad (39)$$

$$\tau_1 = -\frac{q_2}{q_1} \hat{M}K_3^{-1} \tilde{v}^{2-q_1/q_2} \quad (40)$$

$$\tau_2 = \begin{cases} -\frac{(s_v^T K_3 \text{diag}(\tilde{v}^{q_1/q_2-1}) \hat{M}^{-1})^T}{\|s_v^T K_3 \text{diag}(\tilde{v}^{q_1/q_2-1}) \hat{M}^{-1}\|^2} \Omega, \\ \quad \text{for } \|s_v\| \neq 0 \text{ with } \|\tilde{v}\| \neq 0 \\ 0, \quad \text{for } \|s_v\| = 0 \text{ or } \|s_v\| \neq 0 \text{ with } \|\tilde{v}\| = 0 \end{cases} \quad (41)$$

with

$$\Omega = \|s_v\| \|K_3 \text{diag}(\tilde{v}^{q_1/q_2-1}) \hat{M}^{-1}\| (\hat{\lambda}_0 + \hat{\lambda}_1 \|v\| + \hat{\lambda}_2 \|v\|^2) \quad (42)$$

in which $\hat{\lambda}_i (i = 0, 1, 2)$ are the estimates of $\lambda_i (i = 0, 1, 2)$ and they are updated by the following adaptation laws:

$$\dot{\hat{\lambda}}_0 = \chi_0 \frac{q_1}{q_2} \|s_v\| \|K_3 \text{diag}(\tilde{v}^{q_1/q_2-1}) \hat{M}^{-1}\| \quad (43)$$

$$\dot{\hat{\lambda}}_1 = \chi_1 \frac{q_1}{q_2} \|s_v\| \|K_3 \text{diag}(\tilde{v}^{q_1/q_2-1}) \hat{M}^{-1}\| \|v\| \quad (44)$$

$$\dot{\hat{\lambda}}_2 = \chi_2 \frac{q_1}{q_2} \|s_v\| \|K_3 \text{diag}(\tilde{v}^{q_1/q_2-1}) \hat{M}^{-1}\| \|v\|^2 \quad (45)$$

where $\chi_i (i = 0, 1, 2)$ are positive constants that determine the rate of adaptation, and $\hat{\lambda}_i(0) > 0$ for all $i = 0, 1, 2$, then the velocity tracking errors \tilde{v} will locally converge to zero in finite time, and after that the position tracking errors $\tilde{\eta}$ will locally converge to zero exponentially.

The block diagram of the ANITSMC of an AUV is shown in Fig. 2.

4.3 Stability analysis

To prove Theorem 2, the following lemma is needed and is firstly proved.

Lemma 3: Given the AUV dynamic system (31) with the NITSM variable vector s_v (37) controlled by (38)–(45), the gains $\hat{\lambda}_i (i = 0, 1, 2)$ in τ_2 (see (41) and (42)) have upper bounds, i.e. there exist positive constants $\lambda_i^\# (i = 0, 1, 2)$ such that

$$\hat{\lambda}_i \leq \lambda_i^\#, \quad i = 0, 1, 2. \quad (46)$$

Proof: Similar to the proof of Lemma 2 given in Section 3.2, the proof of this lemma is also based on the proof of Lemma 1 of [33]. Suppose that $\tilde{v} \neq 0$ and $s_v \neq 0$, from the update laws of $\hat{\lambda}_i (i = 0, 1, 2)$ expressed in (43)–(45), and given that $\lambda_i (i = 0, 1, 2)$ are bounded, it follows that $\hat{\lambda}_i (i = 0, 1, 2)$ are increasing and there exists a time \bar{t}_1 such that $\hat{\lambda}_i(\bar{t}_1) > \lambda_i$ for $i = 0, 1, 2$. Note that these gains have finite values by the absolute continuity property of $\hat{\lambda}_i (i = 0, 1, 2)$. From $t = \bar{t}_1$, the gains $\hat{\lambda}_i (i = 0, 1, 2)$ are large enough to make the NITSM variable vector s_v decreasing. Then, it yields that, in a finite time \bar{t}_2 , $s_v(\bar{t}_2) = 0$ and $\hat{\lambda}_i(\bar{t}_2) (i = 0, 1, 2)$ admit bounded values. It yields that there always exist positive constants $\lambda_i^\# (i = 0, 1, 2)$ such that $\lambda_i^\# \geq \hat{\lambda}_i$ for $i = 0, 1, 2$. On the other hand, for the case of $\tilde{v} = 0$ and $s_v \neq 0$, from (31) and (36) we have

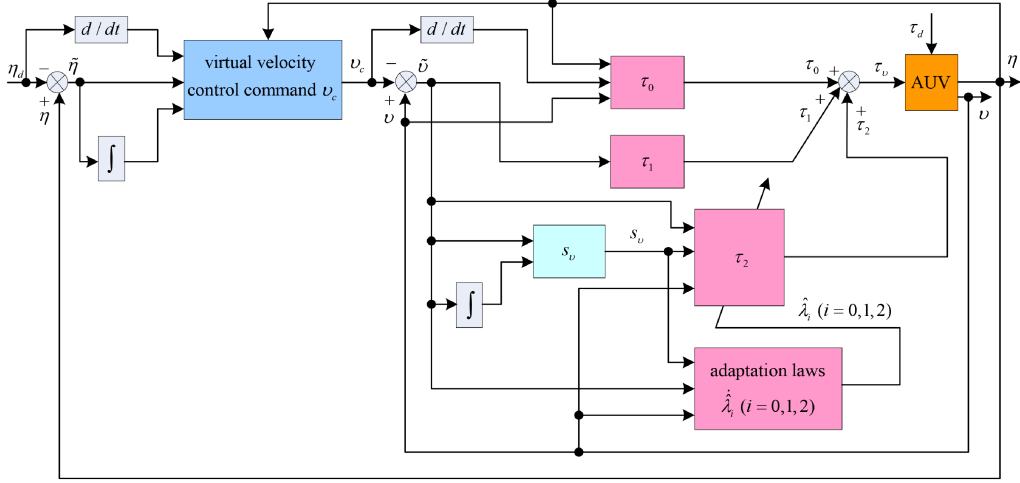


Fig. 2 Block diagram of the ANITSMC of an AUV

$$\begin{aligned} \dot{\tilde{v}} &= \dot{v} - \dot{v}_c \\ &= \hat{M}^{-1}(\tau_v + \tau_{d\eta} - \hat{C}(v)v - \hat{D}(v)v - \hat{g}(\eta)) - \dot{v}_c. \end{aligned} \quad (47)$$

Substituting the control law (38)–(42) into (47) yields

$$\dot{\tilde{v}} = \hat{M}^{-1}\tau_{d\eta}. \quad (48)$$

Assume that $\tilde{v} \equiv 0$, from (32) and (48) we have $\dot{\tilde{v}} \not\equiv 0$ and consequently $\tilde{v} \not\equiv 0$, which is in contradiction with the initial assumption of $\tilde{v} \equiv 0$. Therefore, we obtain $\tilde{v} \not\equiv 0$, showing that $\tilde{v} = 0$ does not hinder the reachability of the NITSM manifold $s_v = 0$. Thus, the gains $\hat{\lambda}_i$ ($i = 0, 1, 2$) will continue to increase until the NITSM variable vector s_v converges to zero. After that, $\hat{\lambda}_i$ ($i = 0, 1, 2$) will admit bounded values and consequently, the boundedness of $\hat{\lambda}_i$ ($i = 0, 1, 2$) is guaranteed, i.e. the inequalities (46) hold for some positive constants λ_i^* ($i = 0, 1, 2$). This completes the proof. \square

With Lemmas 1 and 3 given above, now the proof of Theorem 2 is ready to be given.

Proof of Theorem 2: From Lemma 3, there always exist positive constants λ_i^* ($i = 0, 1, 2$) such that $\lambda_i^* > \lambda_i$ and $\lambda_i^* > \hat{\lambda}_i$ for all $i = 0, 1, 2$. Let $\tilde{\lambda}_i = \hat{\lambda}_i - \lambda_i^*$ for $i = 0, 1, 2$, inspired by [33], consider the following Lyapunov function

$$V = \frac{1}{2}s_v^T s_v + \frac{1}{2} \sum_{i=0}^2 \varphi_i^{-1} \tilde{\lambda}_i^2 \quad (49)$$

where φ_i ($i = 0, 1, 2$) are positive constants satisfying $\varphi_i < \chi_i$.

Differentiating V with respect to time, and substituting (31), (36) and (37) into it yields

$$\begin{aligned} \dot{V} &= s_v^T \dot{s}_v + \sum_{i=0}^2 \varphi_i^{-1} \tilde{\lambda}_i \dot{\tilde{\lambda}}_i \\ &= s_v^T \left(\tilde{v} + \frac{q_1}{q_2} K_3 \text{diag}(\tilde{v}^{q_1/q_2-1}) (\dot{v} - \dot{v}_c) \right) + \sum_{i=0}^2 \varphi_i^{-1} \tilde{\lambda}_i \dot{\tilde{\lambda}}_i \\ &= s_v^T \left(\tilde{v} + \frac{q_1}{q_2} K_3 \text{diag}(\tilde{v}^{q_1/q_2-1}) (\hat{M}^{-1}(\tau_v + \tau_{d\eta}) \right. \\ &\quad \left. - \hat{C}(v)v - \hat{D}(v)v - \hat{g}(\eta) - \dot{v}_c) \right) + \sum_{i=0}^2 \varphi_i^{-1} \tilde{\lambda}_i \dot{\tilde{\lambda}}_i. \end{aligned} \quad (50)$$

Using (38)–(40) in (50) gives

$$\dot{V} = \frac{q_1}{q_2} s_v^T K_3 \text{diag}(\tilde{v}^{q_1/q_2-1}) \hat{M}^{-1} (\tau_2 + \tau_{d\eta}) + \sum_{i=0}^2 \varphi_i^{-1} \tilde{\lambda}_i \dot{\tilde{\lambda}}_i. \quad (51)$$

For the case of $\tilde{v} \neq 0$ and $s_v \neq 0$, utilising $\tilde{\lambda}_i = \hat{\lambda}_i$ ($i = 0, 1, 2$) and substituting (41)–(45) into (51) yields

$$\begin{aligned} \dot{V} &= -\frac{q_1}{q_2} \| s_v \| \| K_3 \text{diag}(\tilde{v}^{q_1/q_2-1}) \hat{M}^{-1} \| \\ &\quad \times (\hat{\lambda}_0 + \hat{\lambda}_1 \| v \| + \hat{\lambda}_2 \| v \|^2) \\ &\quad + \frac{q_1}{q_2} s_v^T K_3 \text{diag}(\tilde{v}^{q_1/q_2-1}) \hat{M}^{-1} \tau_{d\eta} \\ &\quad + \frac{q_1}{q_2} \| s_v \| \| K_3 \text{diag}(\tilde{v}^{q_1/q_2-1}) \hat{M}^{-1} \| (\varphi_0^{-1} \chi_0 (\hat{\lambda}_0 - \lambda_0^*) \\ &\quad + \varphi_1^{-1} \chi_1 (\hat{\lambda}_1 - \lambda_1^*) \| v \| + \varphi_2^{-1} \chi_2 (\hat{\lambda}_2 - \lambda_2^*) \| v \|^2) \end{aligned} \quad (52a)$$

$$\begin{aligned} &\leq -\frac{q_1}{q_2} \| s_v \| \| K_3 \text{diag}(\tilde{v}^{q_1/q_2-1}) \hat{M}^{-1} \| \\ &\quad \times (\hat{\lambda}_0 + \hat{\lambda}_1 \| v \| + \hat{\lambda}_2 \| v \|^2) \\ &\quad + \frac{q_1}{q_2} \| s_v \| \| K_3 \text{diag}(\tilde{v}^{q_1/q_2-1}) \hat{M}^{-1} \| \| \tau_{d\eta} \| \\ &\quad + \frac{q_1}{q_2} \| s_v \| \| K_3 \text{diag}(\tilde{v}^{q_1/q_2-1}) \hat{M}^{-1} \| (\varphi_0^{-1} \chi_0 (\hat{\lambda}_0 - \lambda_0^*) \\ &\quad + \varphi_1^{-1} \chi_1 (\hat{\lambda}_1 - \lambda_1^*) \| v \| + \varphi_2^{-1} \chi_2 (\hat{\lambda}_2 - \lambda_2^*) \| v \|^2) \end{aligned} \quad (52b)$$

$$\begin{aligned} &\leq -\frac{q_1}{q_2} \| s_v \| \| K_3 \text{diag}(\tilde{v}^{q_1/q_2-1}) \hat{M}^{-1} \| \\ &\quad \times (\hat{\lambda}_0 + \hat{\lambda}_1 \| v \| + \hat{\lambda}_2 \| v \|^2) \\ &\quad + \frac{q_1}{q_2} \| s_v \| \| K_3 \text{diag}(\tilde{v}^{q_1/q_2-1}) \hat{M}^{-1} \| \\ &\quad \times (\lambda_0^* + \lambda_1^* \| v \| + \lambda_2^* \| v \|^2) \\ &\quad - \frac{q_1}{q_2} \| s_v \| \| K_3 \text{diag}(\tilde{v}^{q_1/q_2-1}) \hat{M}^{-1} \| \\ &\quad \times (\lambda_0^* + \lambda_1^* \| v \| + \lambda_2^* \| v \|^2) \\ &\quad + \frac{q_1}{q_2} \| s_v \| \| K_3 \text{diag}(\tilde{v}^{q_1/q_2-1}) \hat{M}^{-1} \| \\ &\quad \times (\lambda_0 + \lambda_1 \| v \| + \lambda_2 \| v \|^2) \\ &\quad + \frac{q_1}{q_2} \| s_v \| \| K_3 \text{diag}(\tilde{v}^{q_1/q_2-1}) \hat{M}^{-1} \| (\varphi_0^{-1} \chi_0 (\hat{\lambda}_0 - \lambda_0^*) \\ &\quad + \varphi_1^{-1} \chi_1 (\hat{\lambda}_1 - \lambda_1^*) \| v \| + \varphi_2^{-1} \chi_2 (\hat{\lambda}_2 - \lambda_2^*) \| v \|^2) \end{aligned} \quad (52c)$$

$$\begin{aligned}
&= -\frac{q_1}{q_2} \| s_v \| \| K_3 \text{diag}(\tilde{v}^{q_1/q_2-1}) \hat{M}^{-1} \| ((\lambda_0^* - \lambda_0) \\
&\quad + (\lambda_1^* - \lambda_1) \| v \| + (\lambda_2^* - \lambda_2) \| v \|^2) \\
&\quad + \frac{q_1}{q_2} \| s_v \| \| K_3 \text{diag}(\tilde{v}^{q_1/q_2-1}) \hat{M}^{-1} \| ((\lambda_0^* - \hat{\lambda}_0) \\
&\quad + (\lambda_1^* - \hat{\lambda}_1) \| v \| + (\lambda_2^* - \hat{\lambda}_2) \| v \|^2) \\
&\quad - \frac{q_1}{q_2} \| s_v \| \| K_3 \text{diag}(\tilde{v}^{q_1/q_2-1}) \hat{M}^{-1} \| (\varphi_0^{-1} \chi_0 (\lambda_0^* - \hat{\lambda}_0) \\
&\quad + \varphi_1^{-1} \chi_1 (\lambda_1^* - \hat{\lambda}_1) \| v \| + \varphi_2^{-1} \chi_2 (\lambda_2^* - \hat{\lambda}_2) \| v \|^2)
\end{aligned} \tag{52d}$$

$$\begin{aligned}
&= -\frac{q_1}{q_2} \| K_3 \text{diag}(\tilde{v}^{q_1/q_2-1}) \hat{M}^{-1} \| ((\lambda_0^* - \lambda_0) + (\lambda_1^* - \lambda_1) \| v \| \\
&\quad + (\lambda_2^* - \lambda_2) \| v \|^2) \| s_v \| \\
&\quad - \frac{q_1}{q_2} \| s_v \| \| K_3 \text{diag}(\tilde{v}^{q_1/q_2-1}) \hat{M}^{-1} \| \\
&\quad \times (\varphi_0^{-1} \chi_0 - 1) (\lambda_0^* - \hat{\lambda}_0) \\
&\quad - \frac{q_1}{q_2} \| s_v \| \| K_3 \text{diag}(\tilde{v}^{q_1/q_2-1}) \hat{M}^{-1} \| \\
&\quad \times (\varphi_1^{-1} \chi_1 - 1) \| v \| (\lambda_1^* - \hat{\lambda}_1) \\
&\quad - \frac{q_1}{q_2} \| s_v \| \| K_3 \text{diag}(\tilde{v}^{q_1/q_2-1}) \hat{M}^{-1} \| \\
&\quad \times (\varphi_2^{-1} \chi_2 - 1) \| v \|^2 (\lambda_2^* - \hat{\lambda}_2)
\end{aligned} \tag{52e}$$

here Assumption 4 has been used.

Define

$$\begin{aligned}
\varepsilon_1 &= \frac{q_1}{q_2} \| K_3 \text{diag}(\tilde{v}^{q_1/q_2-1}) \hat{M}^{-1} \| ((\lambda_0^* - \lambda_0) + (\lambda_1^* - \lambda_1) \| v \| \\
&\quad + (\lambda_2^* - \lambda_2) \| v \|^2), \\
\varepsilon_2 &= \frac{q_1}{q_2} \| s_v \| \| K_3 \text{diag}(\tilde{v}^{q_1/q_2-1}) \hat{M}^{-1} \| (\varphi_0^{-1} \chi_0 - 1), \\
\varepsilon_3 &= \frac{q_1}{q_2} \| s_v \| \| K_3 \text{diag}(\tilde{v}^{q_1/q_2-1}) \hat{M}^{-1} \| (\varphi_1^{-1} \chi_1 - 1) \| v \|,
\end{aligned} \tag{53}$$

$$\varepsilon_4 = \frac{q_1}{q_2} \| s_v \| \| K_3 \text{diag}(\tilde{v}^{q_1/q_2-1}) \hat{M}^{-1} \| (\varphi_2^{-1} \chi_2 - 1) \| v \|^2.$$

Then, from (49), (52) and (53) we have

$$\begin{aligned}
\dot{V} &\leq -\sqrt{2}\varepsilon_1 \frac{\sqrt{2}}{2} \| s_v \| - \sqrt{2\varphi_0} \varepsilon_2 \frac{\sqrt{2}}{2\sqrt{\varphi_0}} (\lambda_0^* - \hat{\lambda}_0) \\
&\quad - \sqrt{2\varphi_1} \varepsilon_3 \frac{\sqrt{2}}{2\sqrt{\varphi_1}} (\lambda_1^* - \hat{\lambda}_1) - \sqrt{2\varphi_2} \varepsilon_4 \frac{\sqrt{2}}{2\sqrt{\varphi_2}} (\lambda_2^* - \hat{\lambda}_2) \\
&\leq -\min(\sqrt{2}\varepsilon_1, \sqrt{2\varphi_0}\varepsilon_2, \sqrt{2\varphi_1}\varepsilon_3, \sqrt{2\varphi_2}\varepsilon_4) \left(\frac{\sqrt{2}}{2} \| s_v \| \right. \\
&\quad \left. + \frac{\sqrt{2}}{2\sqrt{\varphi_0}} (\lambda_0^* - \hat{\lambda}_0) + \frac{\sqrt{2}}{2\sqrt{\varphi_1}} (\lambda_1^* - \hat{\lambda}_1) + \frac{\sqrt{2}}{2\sqrt{\varphi_2}} (\lambda_2^* - \hat{\lambda}_2) \right) \\
&\leq -\varepsilon_0 V^{1/2}
\end{aligned} \tag{54}$$

where

$$\varepsilon_0 = \min(\sqrt{2}\varepsilon_1, \sqrt{2\varphi_0}\varepsilon_2, \sqrt{2\varphi_1}\varepsilon_3, \sqrt{2\varphi_2}\varepsilon_4) > 0.$$

Thus, according to Lemma 1, the NITSM manifold $s_v = 0$ can be reached in the finite time

$$t_{\text{reach}} \leq \frac{2V^{1/2}|_{t=0}}{\varepsilon_0}. \tag{55}$$

For the case of $\tilde{v} = 0$ and $s_v \neq 0$, it has been shown in the proof of Lemma 3 that $\tilde{v} = 0$ is not an attractor in the reaching phase. Hence, the reachability of the NITSM manifold $s_v = 0$ in the finite time (55) is still guaranteed.

On the NITSM manifold $s_v = 0$, there is $\int_0^t \tilde{v} d\tau = -K_3 \tilde{v}^{q_1/q_2}$, namely, $\int_0^t \tilde{v}_i d\tau = -k_{3i} \tilde{v}_i^{q_1/q_2}$, $i = 1, \dots, 6$. Then, according to the proof of Theorem 1, the convergent time t_{ci} taken from $\tilde{v}_i(t_{\text{reach}})$ to $\tilde{v}_i(t_{\text{reach}} + t_{ci}) = 0$ for $i = 1, \dots, 6$ can be obtained as

$$t_{ci} = \frac{k_{3i} |\tilde{v}_i(t_{\text{reach}})|^{q_1/q_2-1}}{(1 - q_2/q_1)}, \quad i = 1, \dots, 6. \tag{56}$$

Thus, the total convergent time t_{sum} spent from $\tilde{v}(0)$ to $\tilde{v}(t_{\text{sum}}) = 0$ will be the sum of t_{reach} and $\max_{i=1,\dots,6} (t_{ci})$, i.e.

$$t_{\text{sum}} = t_{\text{reach}} + \max_{i=1,\dots,6} (t_{ci}). \tag{57}$$

From the above proof, it is concluded that the velocity tracking errors \tilde{v} converge to zero in finite time.

When $t \geq t_{\text{sum}}$, we have $\tilde{v} = 0$. It follows from (36) that

$$v = v_c. \tag{58}$$

From (27) and (35), it can be obtained that

$$J^{-1}(\eta) \dot{\eta} = J^{-1}(\eta) \dot{\eta}_d - J^{-1}(\eta) (K_1 \tilde{\eta} + K_2 \int_0^t \tilde{\eta} d\tau) \tag{59}$$

namely

$$\dot{\tilde{\eta}} + K_1 \tilde{\eta} + K_2 \int_0^t \tilde{\eta} d\tau = 0 \tag{60}$$

namely

$$\dot{\tilde{\eta}}_i + k_{1i} \tilde{\eta}_i + k_{2i} \int_0^t \tilde{\eta}_i d\tau = 0, \quad i = 1, \dots, 6. \tag{61}$$

Let $\tilde{\eta}_{ii} = \int_0^t \tilde{\eta}_i d\tau$, then (61) can be written as the following second-order homogeneous differential equation

$$\ddot{\tilde{\eta}}_{ii} + k_{1i} \dot{\tilde{\eta}}_{ii} + k_{2i} \tilde{\eta}_{ii} = 0, \quad i = 1, \dots, 6. \tag{62}$$

Let r_{1i} and r_{2i} denote two roots of the characteristic equation of the above i th differential equation.

For the case of $k_{1i}^2 - 4k_{2i} = 0$, we have $r_{1i} = r_{2i} = -k_{1i}/2 < 0$. According to the differential equation theory, the i th second-order differential equation of (62) is solved as

$$\tilde{\eta}_{ii} = (c_{1i} + c_{2i}t) e^{-k_{1i}(t-t_{\text{sum}})/2} \tag{63}$$

where c_{1i} and c_{2i} are the constant coefficients.

Hence, $\tilde{\eta}_i$ can be solved using $\tilde{\eta}_i = \dot{\tilde{\eta}}_{ii}$ as

$$\tilde{\eta}_i = \dot{\tilde{\eta}}_{ii} = c_{2i} e^{-k_{1i}(t-t_{\text{sum}})/2} - (k_{1i}(c_{1i} + c_{2i}t)/2) e^{-k_{1i}(t-t_{\text{sum}})/2}. \tag{64}$$

For the case of $k_{1i}^2 - 4k_{2i} > 0$, we have $r_{1i} = (-k_{1i} - \sqrt{k_{1i}^2 - 4k_{2i}})/2 < 0$ and $r_{2i} = (-k_{1i} + \sqrt{k_{1i}^2 - 4k_{2i}})/2 < 0$. Based on the differential equation theory, the i th second-order differential equation of (62) is solved as

$$\tilde{\eta}_{ii} = \bar{c}_{1i} e^{(-k_{1i} - \sqrt{k_{1i}^2 - 4k_{2i}})(t-t_{\text{sum}})/2} + \bar{c}_{2i} e^{(-k_{1i} + \sqrt{k_{1i}^2 - 4k_{2i}})(t-t_{\text{sum}})/2} \tag{65}$$

where \bar{c}_{1i} and \bar{c}_{2i} are the constant coefficients.

Therefore, $\tilde{\eta}_i$ can be solved using $\tilde{\eta}_i = \dot{\tilde{\eta}}_{ii}$ as

$$\begin{aligned} \tilde{\eta}_i &= \dot{\tilde{\eta}}_{ii} = \bar{c}_{1i}((-k_{1i} - \sqrt{k_{1i}^2 - 4k_{2i}})/2)e^{(-k_{1i} - \sqrt{k_{1i}^2 - 4k_{2i}})(t - t_{\text{sum}})/2} \\ &\quad + \bar{c}_{2i}((-k_{1i} + \sqrt{k_{1i}^2 - 4k_{2i}})/2)e^{(-k_{1i} + \sqrt{k_{1i}^2 - 4k_{2i}})(t - t_{\text{sum}})/2}. \end{aligned} \quad (66)$$

From (64) and (66), it is concluded that the position tracking errors $\tilde{\eta}$ converge to zero exponentially after $t \geq t_{\text{sum}}$.

On the other hand, due to Assumption 4 in which the lumped system uncertainty $\tau_{d\eta}$ is assumed to be bounded and it is input related, the velocity tracking errors \tilde{v} are locally stable. Owing to Assumption 2 in which the transformation matrix $J(\eta)$ is assumed to be bounded, the position tracking errors $\tilde{\eta}$ are locally stable. This completes the proof. \square

Remark 6: The characteristics of the ANITSMC of AUVs include: (i) it does not involve any negative fractional power terms, hence the singularity problem in conventional TSMC is avoided; (ii) unlike the GFTSTC [6] which needs the bound information of the parameter perturbation in the controller design, it uses an adaptive mechanism to estimate the unknown parameters of the upper bound of the lumped system uncertainty so that the prior knowledge of the upper bound of the lumped system uncertainty is not required; and (iii) with respect to the GFTSTC [6] and ANTSMC [31] which only ensure the tracking errors to converge to bounded regions in the presence of parameter uncertainties and external disturbances, it guarantees the tracking errors to converge to zero in spite of dynamic uncertainties and time-varying external disturbances, thus the tracking precision is improved.

Remark 7: Noted that the control law (41) is discontinuous across the NITSM manifold $s_v = 0$, which may lead to the chattering phenomenon. To reduce the undesired chattering, the following boundary layer control method can be used to replace the discontinuous control law (41)

$$\tau_2 = \begin{cases} \frac{(s_v^T K_3 \text{diag}(\tilde{v}^{q_1/q_2-1}) \hat{M}^{-1})^T}{\| s_v^T K_3 \text{diag}(\tilde{v}^{q_1/q_2-1}) \hat{M}^{-1} \|} \Omega, & \text{if } \| s_v^T K_3 \text{diag}(\tilde{v}^{q_1/q_2-1}) \hat{M}^{-1} \| \geq \sigma \\ \frac{(s_v^T K_3 \text{diag}(\tilde{v}^{q_1/q_2-1}) \hat{M}^{-1})^T}{\sigma^2} \Omega, & \text{if } \| s_v^T K_3 \text{diag}(\tilde{v}^{q_1/q_2-1}) \hat{M}^{-1} \| < \sigma \text{ with } \| \tilde{v} \| \neq 0 \\ 0, & \text{if } \| \tilde{v} \| = 0 \end{cases} \quad (67)$$

where σ is a positive constant that represents the boundary layer thickness, and Ω is defined in (42). By using the above boundary layer control method, the attractiveness of the boundary layer can be guaranteed. For the region inside the boundaries, the ultimate boundedness of the velocity tracking errors \tilde{v} can be ensured to within any neighbourhood of the boundary layer [21]. Moreover, the ultimate boundedness of the position tracking errors $\tilde{\eta}$ can also be guaranteed. This is because that when the bounded velocity tracking errors $\tilde{v} = \Delta v$ remain due to the adoption of the above boundary layer control method, we have

$$v = v_c + \Delta v. \quad (68)$$

Using (27) and (35) leads to

$$J^{-1}(\eta)\dot{\eta} = J^{-1}(\eta)\dot{\eta}_d - J^{-1}(\eta)(K_1\tilde{\eta} + K_2 \int_0^t \tilde{\eta} d\tau) + \Delta v \quad (69)$$

namely

$$\dot{\tilde{\eta}} + K_1\tilde{\eta} + K_2 \int_0^t \tilde{\eta} d\tau = J(\eta)\Delta v = \xi(\eta, v) \quad (70)$$

namely

$$\dot{\tilde{\eta}}_i + k_{1i}\tilde{\eta}_i + k_{2i} \int_0^t \tilde{\eta}_i d\tau = \xi_i, \quad i = 1, \dots, 6. \quad (71)$$

Let $\tilde{\eta}_{ii} = \int_0^t \tilde{\eta}_i d\tau$, then (71) can be written as the following second-order non-homogeneous differential equations

$$\ddot{\tilde{\eta}}_i + k_{1i}\dot{\tilde{\eta}}_i + k_{2i}\tilde{\eta}_i = \xi_i, \quad i = 1, \dots, 6. \quad (72)$$

Set $x_{1i} = \tilde{\eta}_{ii}$, $x_{2i} = \dot{\tilde{\eta}}_i$, $x_i = [x_{1i}, x_{2i}]^T$, then (72) can be rewritten as the following second-order systems:

$$\begin{cases} \dot{x}_{1i} = x_{2i} \\ \dot{x}_{2i} = \xi_i - k_{1i}x_{2i} - k_{2i}x_{1i}, \end{cases} \quad i = 1, \dots, 6. \quad (73)$$

Choose the positive definite Lyapunov function as

$$V_i = x_i^T \begin{bmatrix} (k_{1i} + 2k_{2i})/2 & 1/2 \\ 1/2 & 1 \end{bmatrix} x_i, \quad i = 1, \dots, 6 \quad (74)$$

where $k_{1i} > 1/2$, $i = 1, \dots, 6$.

Then, the time derivatives of V_i ($i = 1, \dots, 6$) are

$$\begin{aligned} \dot{V}_i &= (k_{1i} + 2k_{2i})x_{1i}\dot{x}_{1i} + \dot{x}_{1i}x_{2i} + x_{1i}\dot{x}_{2i} + 2x_{2i}\dot{x}_{2i} \\ &= -k_{2i}x_{1i}^2 - (2k_{1i} - 1)x_{2i}^2 + \xi_i(x_{1i} + 2x_{2i}) \\ &\leq -\min(k_{2i}, 2k_{1i} - 1)\|x_i\|^2 + 3\|\xi_i\|\|x_i\| \\ &= -(\min(k_{2i}, 2k_{1i} - 1) - \delta_i)\|x_i\|^2 - \delta_i\|x_i\|^2 \\ &\quad + 3\|\xi_i\|\|x_i\|, \quad i = 1, \dots, 6 \end{aligned} \quad (75)$$

in which $0 < \delta_i < \min(k_{2i}, 2k_{1i} - 1)$, $i = 1, \dots, 6$. Due to Assumption 2 and the boundedness of the velocity tracking errors Δv , it can be obtained that $\xi(\eta, v) = J(\eta)\Delta v$ are bounded, and consequently ξ_i ($i = 1, \dots, 6$) are bounded. Suppose that ζ_i is the upper bound of ξ_i for $i = 1, \dots, 6$, i.e. $|\xi_i| \leq \zeta_i$ where $\zeta_i > 0$ is a constant, then we can obtain that

$$\begin{aligned} \dot{V}_i &\leq -(\min(k_{2i}, 2k_{1i} - 1) - \delta_i)\|x_i\|^2 \\ &\quad - \delta_i\|x_i\|^2 + 3\zeta_i\|x_i\| \\ &\leq -(\min(k_{2i}, 2k_{1i} - 1) - \delta_i)\|x_i\|^2 \text{ for} \\ &\quad \|x_i\| \geq \frac{3\zeta_i}{\delta_i}, \quad i = 1, \dots, 6. \end{aligned} \quad (76)$$

Equation (76) implies that x_i ($i = 1, \dots, 6$) are bounded. It follows that x_{1i} and x_{2i} ($i = 1, \dots, 6$) are bounded. Due to that $x_{2i} = \dot{\tilde{\eta}}_i = \tilde{\eta}_i$, $i = 1, \dots, 6$, therefore, it is concluded that the position tracking errors $\tilde{\eta}$ are bounded.

Remark 8: If $q_1/q_2 = 1$, the proposed NITSM manifold s_v in (37) will reduce to the conventional proportional-integral sliding mode (PISM) manifold $s_v = \int_0^t \tilde{v} d\tau + K_3 \tilde{v}$. Correspondingly, the designed ANITSMC scheme will reduce to the APISM scheme which is described as

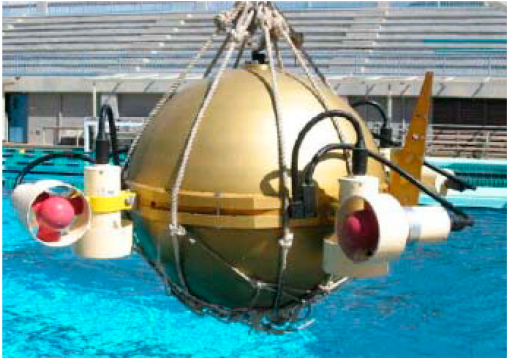


Fig. 3 ODIN AUV

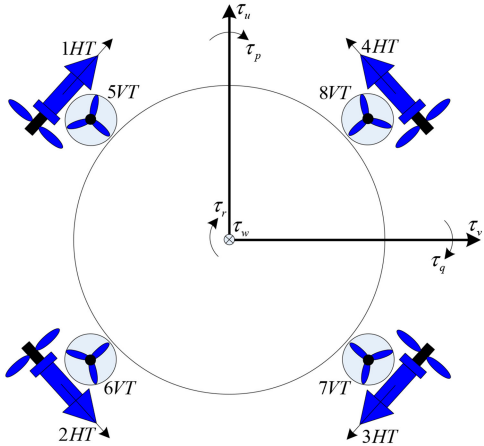


Fig. 4 Thruster layout of the ODIN

$$\begin{aligned} \tau_v &= \tau_0 + \tau_1 + \tau_2, \\ \tau_0 &= \hat{M}\dot{v}_c + \hat{C}(v)v + \hat{D}(v)v + \hat{g}(\eta), \\ \tau_1 &= -\hat{M}K_3^{-1}\tilde{v}, \\ \tau_2 &= \begin{cases} -\frac{(s_v^T K_3 \hat{M}^{-1})^T}{\| s_v^T K_3 \hat{M}^{-1} \|^2} \Omega, & \text{for } \| s_v \| \neq 0 \\ 0, & \text{for } \| s_v \| = 0, \end{cases} \quad (77) \\ \Omega &= \| s_v \| \| K_3 \hat{M}^{-1} \| (\hat{\lambda}_0 + \hat{\lambda}_1 \| v \| + \hat{\lambda}_2 \| v \|^2), \\ \dot{\hat{\lambda}}_0 &= \chi_0 \| s_v \| \| K_3 \hat{M}^{-1} \|, \\ \dot{\hat{\lambda}}_1 &= \chi_1 \| s_v \| \| K_3 \hat{M}^{-1} \| \| v \|, \\ \dot{\hat{\lambda}}_2 &= \chi_2 \| s_v \| \| K_3 \hat{M}^{-1} \| \| v \|^2. \end{aligned}$$

Similar to the proof of Theorem 2, it can be verified that, under the APISM scheme, the position and velocity tracking errors $\tilde{\eta}$ and \tilde{v} will locally asymptotically converge to zero. Correspondingly, the boundary layer control method used to weaken the chattering effects is given by

$$\tau_2 = \begin{cases} -\frac{(s_v^T K_3 \hat{M}^{-1})^T}{\| s_v^T K_3 \hat{M}^{-1} \|^2} \Omega, & \text{if } \| s_v^T K_3 \hat{M}^{-1} \| \geq \sigma \\ -\frac{(s_v^T K_3 \hat{M}^{-1})^T}{\sigma^2} \Omega, & \text{if } \| s_v^T K_3 \hat{M}^{-1} \| < \sigma. \end{cases} \quad (78)$$

Like the analysis in Remark 7, if the boundary layer control method (78) is utilised, the ultimate boundedness of the position and velocity tracking errors $\tilde{\eta}$ and \tilde{v} will be obtained. Compared with this APISM, the proposed ANITSMC provides faster convergence rate and better robustness against dynamic uncertainties and time-varying external disturbances for trajectory

tracking control of AUVs. This is mainly because that the ANITSMC guarantees finite-time convergence of the velocity tracking errors \tilde{v} and it has been shown in [38, 39] that the control system with finite-time convergence can exhibit not only faster convergence rate but also better disturbances rejection ability and better robustness against uncertainties than the control system with asymptotical convergence. The improved performances of the ANITSMC over the APISM can also be seen from the numerical simulations in the following section.

5 Numerical simulations

In this section, numerical simulations are performed to demonstrate the effectiveness of the proposed ANITSMC scheme. A comparison between the APISM given in Remark 8 and the ANITSMC proposed in this study is carried out. To suppress the chattering, the boundary layer control methods (67) and (78) are implemented for ANITSMC and APISM, respectively. The AUV system considered in the simulations is the Omni Directional Intelligent Navigator (ODIN) [40]. The ODIN is a near-spherical AUV with radius 0.31 m. Fig. 3 shows its structure. The vehicle has eight thrusters including four horizontal thrusters and four vertical thrusters. A brief sketch of the vehicle's thruster layout is illustrated in Fig. 4. Here we assume that the eight thrusters mounted on the ODIN are the same and the thruster saturation limit for each thruster is taken as ± 150 N like in [41]. The thrust forces from the eight thrusters of ODIN can be obtained by considering the total control forces and moments τ_v from the following formula:

$$\tau_v = Bu_v \quad (79)$$

where $u_v \in R^8$ is the vector containing the thrust force from each of the eight thrusters, and $B \in R^{6 \times 8}$ denotes the thruster configuration matrix of the vehicle and it is available in [40]. The thrust forces from the eight thrusters can be determined using the pseudo-inverse of matrix B as

$$u_v = B^T(BB^T)^{-1}\tau_v \quad (80)$$

where $B^T(BB^T)^{-1}$ is the pseudo-inverse of matrix B .

The dynamic parameters of the ODIN are taken from [40] for conducting the simulations and are not repeated here. To reflect the uncertainties that are present in the vehicle dynamic model, the dynamic parameters used in the two controllers are 20% smaller than those used in vehicle's model. The time-varying external disturbances acting on the vehicle are chosen as

$$\begin{aligned} \tau_{d1} &= 4 + 3\sin(0.3t) \text{ N}, & \tau_{d2} &= 5\sin(0.2t) \text{ N}, \\ \tau_{d3} &= 2 + 4\sin(0.1t) \text{ N}, & \tau_{d4} &= 3 + 2\cos(0.1t) \text{ Nm}, \\ \tau_{d5} &= 4\cos(0.2t) \text{ Nm}, & \tau_{d6} &= 4 + \cos(0.3t) \text{ Nm}. \end{aligned}$$

To illustrate the effectiveness of the proposed ANITSMC scheme more comprehensively, two trajectory tracking cases are investigated: one with a three-dimensional straight-line trajectory tracking and the other with a spatial helical trajectory tracking.

5.1 Three-dimensional straight-line trajectory tracking

In this section, the ODIN is commanded to track a three-dimensional straight-line trajectory. The desired straight-line trajectory in the inertial frame is selected as

Table 1 Control parameters for APISM and ANITSMC

Controller	Control parameters
APISM	$K_1 = \text{diag}(1, 1, 1, 3, 3, 3)$, $K_2 = \text{diag}(0.01, 0.01, 0.01, 0.5, 0.5, 0.5)$, $K_3 = \text{diag}(0.8, 0.8, 0.8, 0.8, 0.8, 0.8)$, $\sigma = 1.5$, $\chi_i = 3$ $(i = 0, 1, 2)$
ANITSMC	$K_1 = \text{diag}(1, 1, 1, 3, 3, 3)$, $K_2 = \text{diag}(0.01, 0.01, 0.01, 0.5, 0.5, 0.5)$, $K_3 = \text{diag}(0.8, 0.8, 0.8, 0.8, 0.8, 0.8)$, $\sigma = 1.5$, $\chi_i = 3$ $(i = 0, 1, 2)$, $q_1 = 5$, $q_2 = 3$

$$\begin{cases} x_d(t) = 0.1t \text{ m} \\ y_d(t) = 0.1t + 0.5 \text{ m} \\ z_d(t) = 0.2t + 1.5 \text{ m} \\ \phi_d(t) = 0 \text{ rad} \\ \theta_d(t) = -\arctan(\sqrt{2}) \text{ rad} \\ \psi_d(t) = \pi/4 \text{ rad}. \end{cases} \quad (81)$$

For both controllers, the initial states of the vehicle are set as $(x(0), y(0), z(0)) = (0.5, 1.1, 1) \text{ m}$, $(\phi(0), \theta(0), \psi(0)) = (0.2, 0, 0.5) \text{ rad}$, $(u(0), v(0), w(0)) = (0, 0, 0) \text{ m/s}$ and $(p(0), q(0), r(0)) = (0, 0, 0) \text{ rad/s}$. The initial values of the adaptive parameters $\hat{\lambda}_i$ ($i = 0, 1, 2$) are chosen as $\hat{\lambda}_i(0) = 0.01$ for $i = 0, 1, 2$. To make the comparison fair and persuasive, corresponding control parameters of the two controllers are selected exactly the same values as shown in Table 1. The simulation results are presented in Figs. 5 and 6.

Fig. 5 shows the three-dimensional straight-line trajectory tracking results under the action of the ANITSMC and APISM. Fig. 5a illustrates the desired and actual trajectories in three-dimensional space. Figs. 5b and c depict the corresponding position and velocity tracking errors, respectively. It can be seen from this figure that under both controllers, the ODIN successfully tracks the desired trajectory and the position and velocity tracking errors converge to small bounded regions around the origin. However, the convergence rate for the ANITSMC is faster than that for the APISM. Moreover, the bounds of the steady-state position and velocity tracking errors under the ANITSMC are smaller than those under the APISM, which implies that the ANITSMC offers better robustness against dynamic uncertainties and time-varying external disturbances for the AUV dynamics.

Fig. 6 displays the thrust forces of the eight thrusters under the ANITSMC and APISM. Figs. 6a and b plot the thrust forces of the eight thrusters under the ANITSMC. Figs. 6c and d plot the thrust forces of the eight thrusters under the APISM. As can be seen from this figure, by using the boundary layer control methods, the chattering is effectively weakened for both controllers. In addition, the thrust force of each thruster only violates its saturation limit in the beginning phase, thus (33) is valid.

5.2 Spatial helical trajectory tracking

In this section, the ODIN is commanded to track a spatial helical trajectory. The desired helical trajectory in the inertial frame is chosen as

$$\begin{cases} x_d(t) = \sin(0.2t) \text{ m} \\ y_d(t) = \cos(0.2t) \text{ m} \\ z_d(t) = 0.1t + 1 \text{ m} \\ \phi_d(t) = 0 \text{ rad} \\ \theta_d(t) = -\arctan(1/2) \text{ rad} \\ \psi_d(t) = 0.2t \text{ rad}. \end{cases} \quad (82)$$

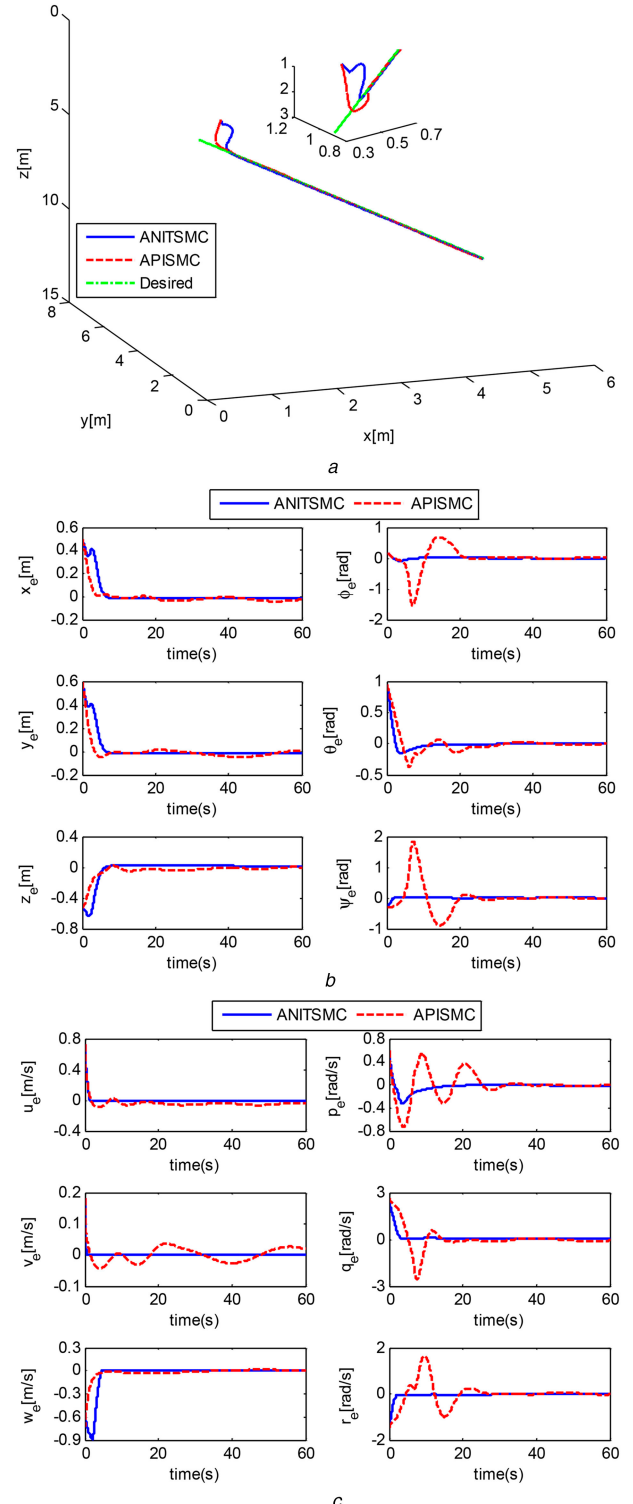


Fig. 5 Three-dimensional straight-line trajectory tracking results under ANITSMC and APISM
(a) Three-dimensional phase plot, (b) Position tracking errors, (c) Velocity tracking errors

For both controllers, the initial states of the vehicle are set as $(x(0), y(0), z(0)) = (0.4, 1.3, 0.6) \text{ m}$, $(\phi(0), \theta(0), \psi(0)) = (0.1, 0, 0.2) \text{ rad}$, $(u(0), v(0), w(0)) = (0, 0, 0) \text{ m/s}$ and $(p(0), q(0), r(0)) = (0, 0, 0) \text{ rad/s}$. The initial values of the adaptive parameters $\hat{\lambda}_i$ ($i = 0, 1, 2$) are chosen the same as in the three-dimensional straight-line trajectory tracking. The control parameters of the two controllers are the same as those in Table 1 except for replacing the gain matrix K_2 by $K_2 = \text{diag}(0.1, 0.1, 0.01, 0.5, 0.5, 0.5)$. The simulation results are presented in Figs. 7 and 8.

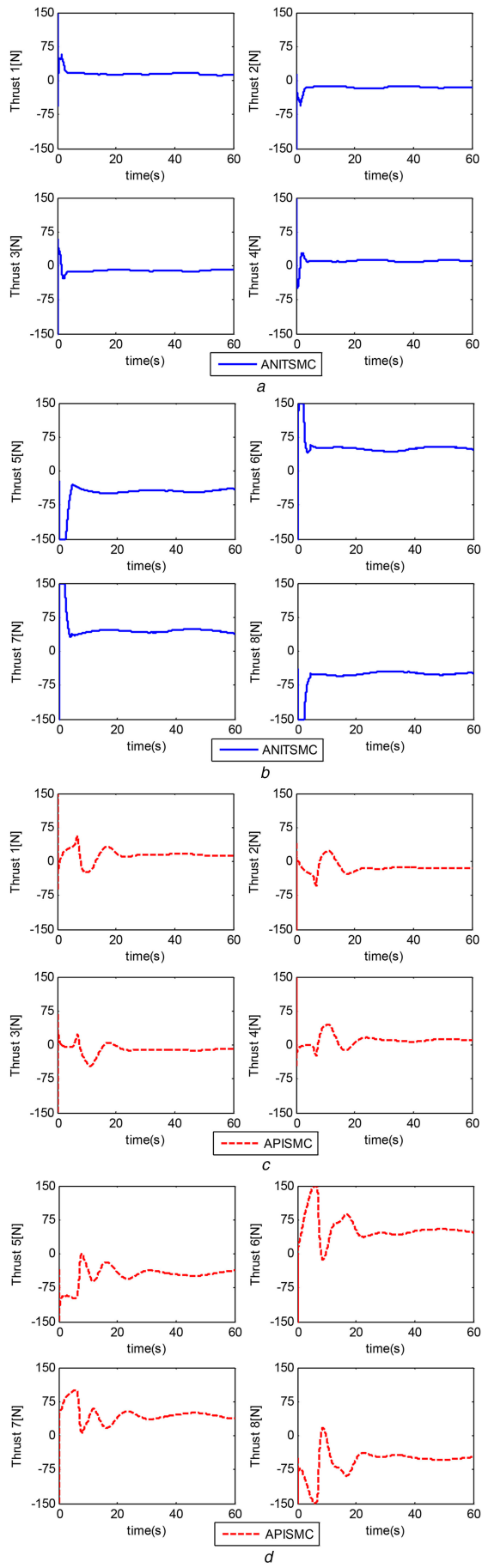


Fig. 6 Thrust forces of the eight thrusters with respect to three-dimensional straight-line trajectory tracking under ANITSMC and APISM
(a) Thrust forces of horizontal thrusters 1–4 under ANITSMC, **(b)** Thrust forces of vertical thrusters 5–8 under ANITSMC, **(c)** Thrust forces of horizontal thrusters 1–4 under APISM, **(d)** Thrust forces of vertical thrusters 5–8 under APISM

1304

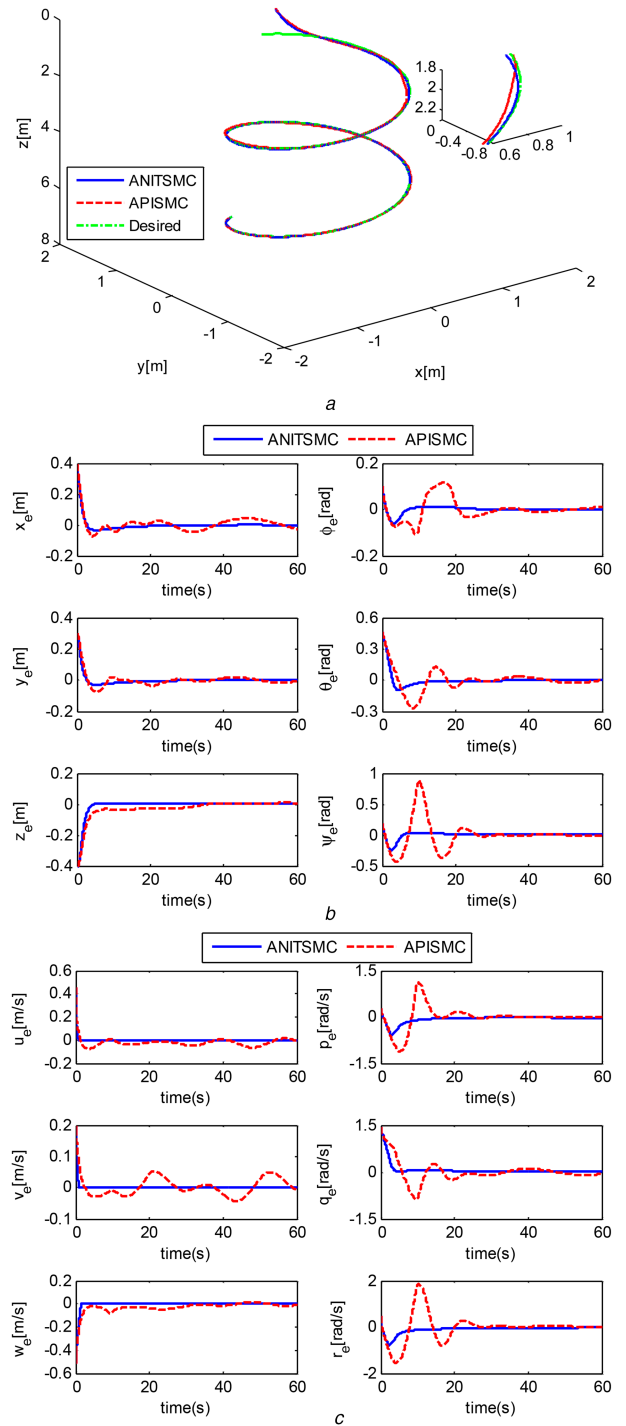


Fig. 7 Spatial helical trajectory tracking results under ANITSMC and APISM
(a) Three-dimensional phase plot, **(b)** Position tracking errors, **(c)** Velocity tracking errors

Fig. 7 illustrates the spatial helical trajectory tracking results under the action of the ANITSMC and APISM. Fig. 7a shows the desired and actual trajectories in three-dimensional space. The position and velocity tracking errors are illustrated in Figs. 7b and c, respectively. As shown by this figure, the ODIN efficiently tracks the desired trajectory and the position and velocity tracking errors converge to small bounded fields. Clearly, the ANITSMC provides faster convergence rate than the APISM, and moreover, the ANITSMC offers smaller bounds of the steady-state position and velocity tracking errors than the APISM, which shows better robustness against dynamic uncertainties and time-varying external disturbances.

Fig. 8 shows the thrust forces of the eight thrusters under the ANITSMC and APISM. The thrust forces of the eight thrusters

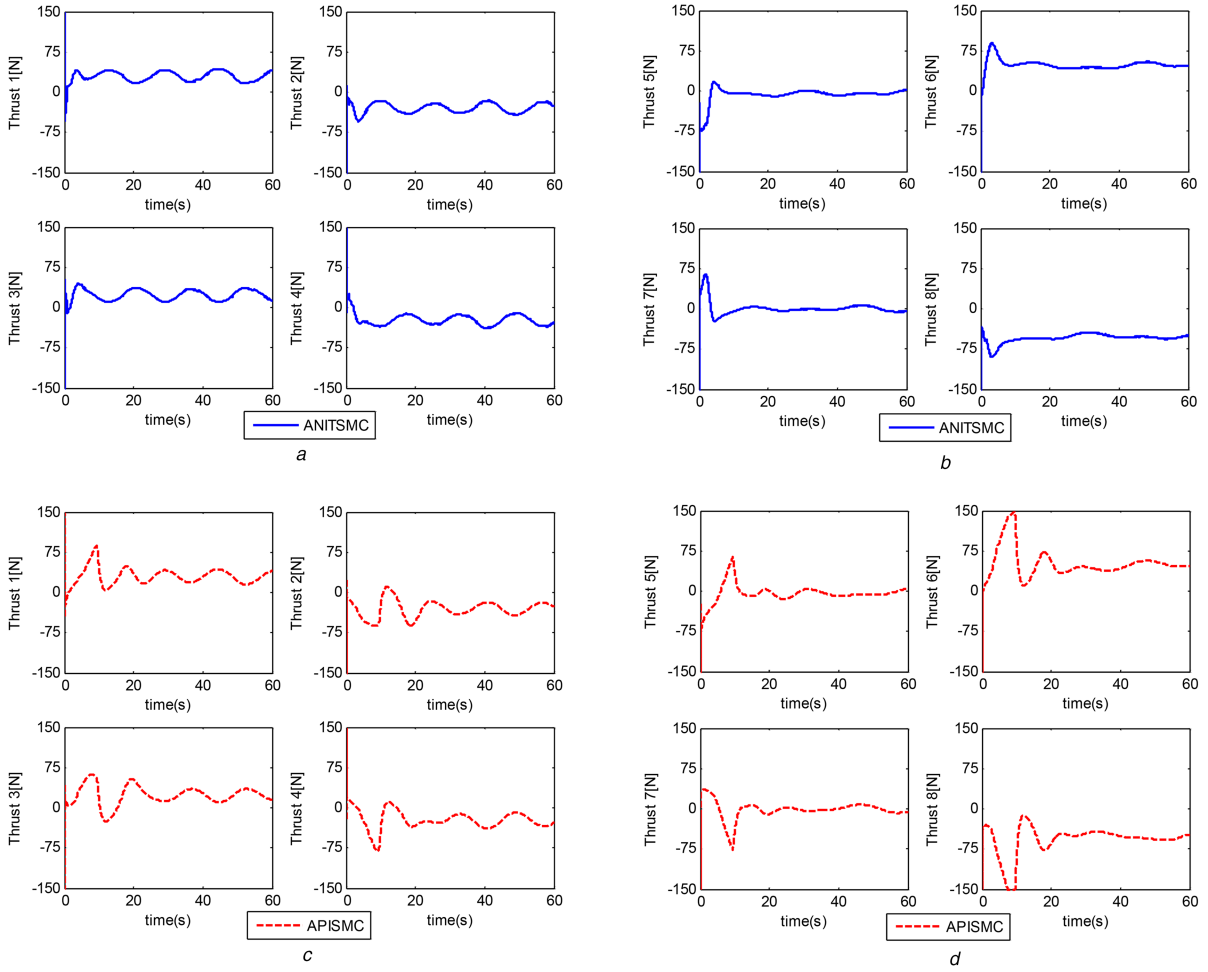


Fig. 8 Thrust forces of the eight thrusters with respect to spatial helical trajectory tracking under ANITSMC and APISMNC

(a) Thrust forces of horizontal thrusters 1–4 under ANITSMC, (b) Thrust forces of vertical thrusters 5–8 under ANITSMC, (c) Thrust forces of horizontal thrusters 1–4 under APISMNC, (d) Thrust forces of vertical thrusters 5–8 under APISMNC

under the ANITSMC are given in Figs. 8a and b and the thrust forces of the eight thrusters under the APISMNC are given in Figs. 8c and d. It can be seen from this figure that chattering is eliminated for both controllers by using the boundary layer control methods. Besides that, the thrust force of each thruster only reaches its saturation limit in the beginning phase, hence, the validity of (33) is verified.

6 Conclusion

In this paper, an ANITSMC scheme is proposed for trajectory tracking of AUVs in the presence of dynamic uncertainties and time-varying external disturbances. The ANITSMC is first implemented for a first-order uncertain non-linear dynamic system to enable the elimination of the singularity problem associated with conventional TSMC and the avoidance of the requirement of the bound information of the lumped system uncertainty. The time taken to reach the equilibrium point from any initial error has been proved to be finite. The proposed ANITSMC has then been used for trajectory tracking control of AUVs. The locally finite-time convergence of the velocity tracking errors to zero is guaranteed, and after that the locally exponential convergence of the position tracking errors to zero is ensured. The contributions of the ANITSMC of AUVs are summarised as follows. First, with comparison to the GFTSTC [6], the ANITSMC does not require the prior knowledge of the upper bound of the lumped system uncertainty. Second, in contrast to the GFTSTC [6] and ANTSMC [31], the ANITSMC provides higher tracking accuracy. Third, compared with the APISMNC, the ANITSMC offers faster convergence rate and better robustness against dynamic uncertainties and time-varying external disturbances. Comparative simulation results verify the improved performances of the ANITSMC over the APISMNC.

7 Acknowledgments

This work is partly supported by the National Natural Science Foundation of China (61473183, 61521063 and U1509211), Program of Shanghai Subject Chief Scientist (14XD1402400).

8 References

- [1] Yuh, J.: ‘Design and control of autonomous underwater robots: a survey’, *Auton. Robots*, 2000, **8**, (1), pp. 7–24
- [2] Xiang, X., Lapierre, L., Jouvel, B.: ‘Smooth transition of AUV motion control: from fully-actuated to under actuated configuration’, *Robot. Auton. Syst.*, 2015, **67**, pp. 14–22
- [3] Santhakumar, M., Asokan, T.: ‘Power efficient dynamic station keeping control of a flat-fish type autonomous underwater vehicle through design modifications of thruster configuration’, *Ocean Eng.*, 2013, **58**, pp. 11–21
- [4] Li, H., Yan, W.: ‘Model predictive stabilization of constrained underactuated autonomous underwater vehicles with guaranteed feasibility and stability’, *IEEE/ASME Trans. Mechatron.*, 2016, online, DOI: 10.1109/TMECH.2016.2587288
- [5] Xu, J., Wang, M., Qiao, L.: ‘Dynamical sliding mode control for the trajectory tracking of underactuated unmanned underwater vehicles’, *Ocean Eng.*, 2015, **105**, pp. 54–63
- [6] Yan, Z., Yu, H., Zhang, W., et al.: ‘Globally finite-time stable tracking control of underactuated UUVs’, *Ocean Eng.*, 2015, **107**, pp. 132–146
- [7] Peng, Z., Wang, D., Wang, H., et al.: ‘Distributed coordinated tracking of multiple autonomous underwater vehicles’, *Nonlinear Dyn.*, 2014, **78**, (2), pp. 1261–1276
- [8] Slotine, J.J., Li, W.: ‘Applied nonlinear control’ (Prentice-Hall, 1991)
- [9] Yang, L., Yang, J.: ‘Nonsingular fast terminal sliding mode control for nonlinear dynamical systems’, *Int. J. Robust Nonlinear Control*, 2011, **21**, (16), pp. 1865–1879
- [10] Cheng, J., Yi, J., Zhao, D.: ‘Design of a sliding mode controller for trajectory tracking problem of marine vessels’, *IET Control Theory Appl.*, 2007, **1**, (1), pp. 233–237
- [11] Soylu, S., Buckham, B.J., Podhorodeski, R.P.: ‘A chattering-free sliding-mode controller for underwater vehicles with fault-tolerant infinity-norm thrust allocation’, *Ocean Eng.*, 2008, **35**, (16), pp. 1647–1659

- [12] Bessa, W.M., Dutra, M.S., Kreuzer, E.: ‘An adaptive fuzzy sliding mode controller for remotely operated underwater vehicles’, *Rob. Autom. Syst.*, 2010, **58**, (1), pp. 16–26
- [13] Zhang, M., Chu, Z.: ‘Adaptive sliding mode control based on local recurrent neural networks for underwater robot’, *Ocean Eng.*, 2012, **45**, pp. 56–62
- [14] Kim, M., Joe, H., Yu, S.: ‘Integral sliding mode controller for precise maneuvering of autonomous underwater vehicle in the presence of unknown environmental disturbances’, *Int. J. Control.*, 2015, **88**, (10), pp. 2055–2065
- [15] Wang, Y., Zhang, M., Wilson, P.A., et al.: ‘Adaptive neural network-based backstepping fault tolerant control for underwater vehicles with thruster fault’, *Ocean Eng.*, 2015, **110**, pp. 15–24
- [16] Qiao, L., Zhang, W.: ‘Double-loop chattering-free adaptive integral sliding mode control for underwater vehicles’. Proc. MTS/IEEE OCEANS Conf., Shanghai, China, April 2016, pp. 1–6
- [17] Cui, R., Zhang, X., Cui, D.: ‘Adaptive sliding-mode attitude control for autonomous underwater vehicles with input nonlinearities’, *Ocean Eng.*, 2016, **123**, pp. 45–54
- [18] Yu, X., Man, Z.: ‘Model reference adaptive control systems with terminal sliding modes’, *Int. J. Control.*, 1996, **64**, (6), pp. 1165–1176
- [19] Man, Z., Yu, X.: ‘Terminal sliding mode control of MIMO linear systems’, *IEEE Trans. Circuits Syst. I: Fundam. Theor. Appl.*, 1997, **44**, (11), pp. 1065–1070
- [20] Wu, Y., Yu, X., Man, Z.: ‘Terminal sliding mode control design for uncertain dynamic systems’, *Syst. Control Lett.*, 1998, **34**, (5), pp. 281–287
- [21] Man, Z., Paplinski, A.P., Wu, H.R.: ‘A robust MIMO terminal sliding mode control for rigid robotic manipulators’, *IEEE Trans. Autom. Control*, 1994, **39**, (12), pp. 2464–2469
- [22] Tang, Y.: ‘Terminal sliding mode control for rigid robots’, *Automatica*, 1998, **34**, (1), pp. 51–56
- [23] Park, K.B., Li, J.J.: ‘Comments on a robust MIMO terminal sliding mode control for rigid robotic manipulators’, *IEEE Trans. Autom. Control*, 1996, **41**, (5), pp. 761–761
- [24] Feng, Y., Yu, X., Man, Z.: ‘Non-singular terminal sliding mode control of rigid manipulators’, *Automatica*, 2002, **38**, (12), pp. 2159–2167
- [25] Yu, S., Yu, X., Shirinzadeh, B.: ‘Continuous finite-time control for robotic manipulators with terminal sliding mode’, *Automatica*, 2005, **41**, (11), pp. 1957–1964
- [26] Jin, M., Lee, J., Chang, P.H., et al.: ‘Practical nonsingular terminal sliding-mode control of robot manipulators for high-accuracy tracking control’, *IEEE Trans. Ind. Electron.*, 2009, **56**, (9), pp. 3593–3601
- [27] Wang, Y., Gu, L., Xu, Y., et al.: ‘Practical tracking control of robot manipulators with continuous fractional-order nonsingular terminal sliding mode’, *IEEE Trans. Ind. Electron.*, 2016, **63**, (10), pp. 6194–6204
- [28] Geng, J., Sheng, Y., Liu, X.: ‘Time-varying nonsingular terminal sliding mode control for robot manipulators’, *Trans. Inst. Meas. Control*, 2014, **36**, (5), pp. 604–617
- [29] Chiu, C.S.: ‘Derivative and integral terminal sliding mode control for a class of MIMO nonlinear systems’, *Automatica*, 2012, **48**, (2), pp. 316–326
- [30] Li, P., Ma, J., Zheng, Z., et al.: ‘Fast nonsingular integral terminal sliding mode control for nonlinear dynamical systems’. Proc. 53rd IEEE Decision Control Conf., Los Angeles, California, USA, December 2014, pp. 4739–4746
- [31] Wang, Y., Gu, L., Gao, M., et al.: ‘Multivariable output feedback adaptive terminal sliding mode control for underwater vehicles’, *Asian. J. Control*, 2016, **18**, (1), pp. 247–265
- [32] Bhat, S.P., Bernstein, D.S.: ‘Continuous finite-time stabilization of the translational and rotational double integrators’, *IEEE Trans. Autom. Control*, 1998, **43**, (5), pp. 678–682
- [33] Plestan, F., Shtessel, Y., Bregeault, V., et al.: ‘New methodologies for adaptive sliding mode control’, *Int. J. Control.*, 2010, **83**, (9), pp. 1907–1919
- [34] Fossen, T.I.: ‘*Guidance and control of ocean vehicles*’ (Wiley, 1994)
- [35] Fischer, N., Hughes, D., Walters, P., et al.: ‘Nonlinear RISE-based control of an autonomous underwater vehicle’, *IEEE Trans. Robotics*, 2014, **30**, (4), pp. 845–852
- [36] Do, K.D., Pan, J.: ‘*Control of ships and underwater vehicles: design for underactuated and nonlinear marine systems*’ (Springer, 2009)
- [37] Zhang, M., Liu, X., Yin, B., et al.: ‘Adaptive terminal sliding mode based thruster fault tolerant control for underwater vehicle in time-varying ocean currents’, *J. Franklin Inst.*, 2015, **352**, (11), pp. 4935–4961
- [38] Li, S., Ding, S., Li, Q.: ‘Global set stabilisation of the spacecraft attitude using finite-time control technique’, *Int. J. Control.*, 2009, **82**, (5), pp. 822–836
- [39] Li, S., Wang, X., Zhang, L.: ‘Finite-time output feedback tracking control for autonomous underwater vehicles’, *IEEE J. Oceanic Eng.*, 2015, **40**, (3), pp. 727–751
- [40] Podder, T.K., Sarkar, N.: ‘Fault-tolerant control of an autonomous underwater vehicle under thruster redundancy’, *Rob. Autom. Syst.*, 2001, **34**, (1), pp. 39–52
- [41] Sarkar, N., Podder, T.K., Antonelli, G.: ‘Fault-accommodating thruster force allocation of an AUV considering thruster redundancy and saturation’, *IEEE Trans. Rob. Autom.*, 2002, **18**, (2), pp. 223–233